

Occurrence and Origin of Andalusite in Peraluminous Felsic Igneous Rocks.

D. Barrie Clarke, Michael Dorais, Bernard Barbarin, Dan Barker, Bernardo Cesare, Geoffrey Clarke, Mohamed El Baghdadi, Saskia Erdmann, Hans-Jürgen Förster, Mario Gaeta, et al.

▶ **To cite this version:**

D. Barrie Clarke, Michael Dorais, Bernard Barbarin, Dan Barker, Bernardo Cesare, et al.. Occurrence and Origin of Andalusite in Peraluminous Felsic Igneous Rocks.. Journal of Petrology, 2005, 46, pp.3, 441-472. 10.1093/petrology/egh083 . hal-00023344

HAL Id: hal-00023344
https://insu.hal.science/hal-00023344

Submitted on 1 Jun 2006

HAL is a multi-disciplinary open access archive for the deposit and dissemination of scientific research documents, whether they are published or not. The documents may come from teaching and research institutions in France or abroad, or from public or private research centers.

L'archive ouverte pluridisciplinaire **HAL**, est destinée au dépôt et à la diffusion de documents scientifiques de niveau recherche, publiés ou non, émanant des établissements d'enseignement et de recherche français ou étrangers, des laboratoires publics ou privés.

Occurrence and Origin of Andalusite in Peraluminous Felsic Igneous Rocks

D. BARRIE CLARKE[1,*], MICHAEL DORAIS[2], BERNARD BARBARIN[3], DAN BARKER[4], BERNARDO CESARE[5], GEOFFREY CLARKE[6], MOHAMED EL BAGHDADI[7], SASKIA ERDMANN[1], HANS-JÜRGEN FÖRSTER[8], MARIO GAETA[9], BÄRBEL GOTTESMANN[8], REBECCA A. JAMIESON[1], DANIEL J. KONTAK[10], FRIEDRICH KOLLER[11], CARLOS LEAL GOMES[12], DAVID LONDON[13], GEORGE B. MORGAN, VI[13], LUIS J. P. F. NEVES[14], DAVID R. M. PATTISON[15], ALCIDES J. S. C. PEREIRA[14], MICHEL PICHAVANT[16], CARLOS W. RAPELA[17], AXEL D. RENNO[18], SIMON RICHARDS[19], MALCOLM ROBERTS[20], ALESSANDRO ROTTURA[21], JULIO SAAVEDRA[22], ALCIDES NOBREGA SIAL[23], ALEJANDRO J. TOSELLI[24], JOSE M. UGIDOS[25], PAVEL UHER[26], CARLOS VILLASECA[27], DARIO VISONÀ[5], DONNA L. WHITNEY[28], BEN WILLIAMSON[29] and HENRY H. WOODARD[30]

[1] DEPARTMENT OF EARTH SCIENCES, DALHOUSIE UNIVERSITY, HALIFAX, NS, CANADA B3H 3J5
[2] DEPARTMENT OF GEOLOGY, BRIGHAM YOUNG UNIVERSITY, PROVO, UT 84602, USA
[3] LABORATOIRE MAGMAS ET VOLCANS, UNIVERSITÉ BLAISE PASCAL, 5 RUE KESSLER, F63038 CLERMONT-FERRAND CEDEX, FRANCE
[4] DEPARTMENT OF GEOLOGICAL SCIENCES, UNIVERSITY OF TEXAS, AUSTIN, TX 78712, USA
[5] DIPARTIMENTO DI MINERALOGIA E PETROLOGIA, UNIVERSITÁ DI PADOVA, I-35137 PADOVA, ITALY
[6] SCHOOL OF GEOSCIENCES, UNIVERSITY OF SYDNEY, SYDNEY, N.S.W. 2006, AUSTRALIA
[7] LABORATOIRE D'EXPLORATION ET GESTION DES RESSOURCES NATURELLES, DÉPARTEMENT DES SCIENCES DE LA TERRE, FACULTÉ DES SCIENCES ET TECHNIQUES, BENI MELLAL, MOROCCO
[8] GEOFORSCHUNGSZENTRUM POTSDAM, D-14473 POTSDAM, GERMANY
[9] UNIVERSITÀ DEGLI STUDI DI ROMA LA SAPIENZA, DIPARTIMENTO DI SCIENZE DELLA TERRA, PIAZZALE ALDO MORO 5, 00185 ROME, ITALY
[10] NOVA SCOTIA DEPARTMENT OF NATURAL RESOURCES, PO BOX 698, HALIFAX, NS, CANADA B3J 2T9
[11] DEPARTMENT OF GEOLOGICAL SCIENCE, UNIVERSITY OF VIENNA, A-1090 VIENNA, AUSTRIA
[12] DEPARTAMENTO DE CIÊNCIAS DA TERRA, UNIVERSIDADE DO MINHO, 4710-057 BRAGA, PORTUGAL
[13] SCHOOL OF GEOLOGY AND GEOPHYSICS, UNIVERSITY OF OKLAHOMA, NORMAN, OK 73019-0628, USA
[14] DEPARTAMENTO DE CIENCIAS DA TERRA, UNIVERSIDADE DE COIMBRA, 3000-272 COIMBRA, PORTUGAL
[15] DEPARTMENT OF GEOLOGY AND GEOPHYSICS, UNIVERSITY OF CALGARY, CALGARY, AB, CANADA T2N 1N4
[16] INSTITUT DES SCIENCES DE LA TERRE D'ORLÉANS (ISTO, UMR 6113), 45071 ORLÉANS CEDEX 2, FRANCE
[17] CENTRO DE INVESTIGACIONES GEOLÓGICAS, 644 CALLE NO. 1, 1900 LA PLATA, ARGENTINA
[18] INSTITUTE OF MINERALOGY, FREIBERG UNIVERSITY, D-09596 FREIBERG, GERMANY
[19] SCHOOL OF GEOSCIENCES, UNIVERSITY OF NEWCASTLE, NEWCASTLE, N.S.W., AUSTRALIA
[20] THE COUNCIL FOR GEOSCIENCE, PO BOX 5347, PORT ELIZABETH 6065, SOUTH AFRICA
[21] DIPARTIMENTO DI SCIENZE DELLA TERRA E GEOLOGICO-AMBIENTALI, UNIVERSITÁ DI BOLOGNA, 40126 BOLOGNA, ITALY
[22] INSTITUTO DE RECURSOS NATURALES Y AGROBIOLOGIA, CSIC, 37071 SALAMANCA, SPAIN
[23] NEG-LABISE, DEPARTMENT OF GEOLOGY, FEDERAL UNIVERSITY OF PERNAMBUCO, RECIFE, PE 50670-000, BRAZIL
[24] UNIVERSIDAD NACIONAL DE TUCUMAN, FACULTAD CIENCIAS NATURALES, INSTITUTO SUPERIOR CORRELACIÓN GEOLÓGICA, 4000 SAN MIGUEL DE TUCUMAN, ARGENTINA
[25] DEPARTAMENTO DE GEOLOGIA, FACULTAD DE CIENCIAS, 37008 SALAMANCA, SPAIN
[26] DEPARTMENT OF MINERAL DEPOSITS, FACULTY OF NATURAL SCIENCES, THE COMENIUS UNIVERSITY, MLYSKA DOLINA G, 842 15 BRATISLAVA, SLOVAKIA
[27] DEPARTAMENTO DE PETROLOGIA Y GEOQUIMICA, FACULTAD DE CC. GEOLOGICAS, UNIVERSIDAD COMPLUTENSE, 28040 MADRID, SPAIN
[28] DEPARTMENT OF GEOLOGY AND GEOPHYSICS, UNIVERSITY OF MINNESOTA, MINNEAPOLIS, MN 55455, USA
[29] DEPARTMENT OF MINERALOGY, THE NATURAL HISTORY MUSEUM, LONDON SW7 5BD, UK
[30] DEPARTMENT OF GEOLOGY, BELOIT COLLEGE, BELOIT, WI 53511, USA

ABSTRACT

Andalusite occurs as an accessory mineral in many types of peraluminous felsic igneous rocks, including rhyolites, aplites, granites, pegmatites, and anatectic migmatites. Some published stability curves for And = Sil and the water-saturated granite solidus permit a small stability field for andalusite in equilibrium with felsic melts. We examine 108 samples of andalusite-bearing felsic rocks from more than 40 localities world-wide. Our purpose is to determine the origin of andalusite, including the *T–P–X* controls on andalusite formation, using eight textural and chemical criteria: size—compatibility with grain sizes of igneous minerals in the same rock; shape—ranging from euhedral to anhedral, with no simple correlation with origin; state of aggregation—single grains or clusters of grains; association with muscovite—with or without rims of monocrystalline or polycrystalline muscovite; inclusions—rare mineral inclusions and melt inclusions; chemical composition—andalusite with little significant chemical variation, except in iron content (0·08–1·71 wt % FeO); compositional zoning—concentric, sector, patchy, oscillatory zoning cryptically reflect growth conditions; compositions of coexisting phases—biotites with high siderophyllite–eastonite contents ($Al^{iv} \approx 2{\cdot}68 \pm 0{\cdot}07$ atoms per formula unit), muscovites with 0·57–4·01 wt % FeO and 0·02–2·85 wt % TiO_2, and apatites with 3·53 ± 0·18 wt % F. Coexisting muscovite–biotite pairs have a wide range of F contents, and $F_{Bt} = 1{\cdot}612F_{Ms} + 0{\cdot}015$. Most coexisting minerals have compositions consistent with equilibration at magmatic conditions. The three principal genetic types of andalusite in felsic igneous rocks are: Type 1 Metamorphic—(a) prograde metamorphic (in thermally metamorphosed peraluminous granites), (b) retrograde metamorphic (inversion from sillimanite of unspecified origin), (c) xenocrystic (derivation from local country rocks), and (d) restitic (derivation from source regions); Type 2 Magmatic—(a) peritectic (water-undersaturated, $T\uparrow$) associated with leucosomes in migmatites, (b) peritectic (water-undersaturated, $T\downarrow$), as reaction rims on garnet or cordierite, (c) cotectic (water-undersaturated, $T-$) direct crystallization from a silicate melt, and (d) pegmatitic (water-saturated, $T\downarrow$), associated with aplite–pegmatite contacts or pegmatitic portion alone; Type 3 Metasomatic—(water-saturated, magma-absent), spatially related to structural discontinuities in host, replacement of feldspar and/or biotite, intergrowths with quartz. The great majority of our andalusite samples show one or more textural or chemical criteria suggesting a magmatic origin. Of the many possible controls on the formation of andalusite (excess Al_2O_3, water concentration and fluid evolution, high Be–B–Li–P, high F, high Fe–Mn–Ti, and kinetic considerations), the two most important factors appear to be excess Al_2O_3 and the effect of releasing water (either to strip alkalis from the melt or to reduce alumina solubility in the melt). Of particular importance is the evidence for magmatic andalusite in granites showing no significant depression of the solidus, suggesting that the And = Sil equilibrium must cross the granite solidus rather than lie below it. Magmatic andalusite, however formed, is susceptible to supra- or sub-solidus reaction to produce muscovite. In many cases, textural evidence of this reaction remains, but in other cases muscovite may completely replace andalusite leaving little or no evidence of its former existence.

KEY WORDS: *andalusite; granite; magmatic; origin; xenocrystic*

INTRODUCTION

Purpose

Andalusite occurs as an accessory mineral in a wide range of felsic peraluminous {A/CNK = molar $[(Al_2O_3)/(CaO + Na_2O + K_2O)] > 1$} extrusive and intrusive igneous rocks. The purposes of this contribution are:

1. to present textural observations and chemical data from a wide range of andalusite-bearing felsic igneous rocks, including fine-grained glassy volcanics, anatectic leucosomes, fine-grained aplites, medium- to coarse-grained granitoids, and very coarse-grained granite pegmatites;
2. to discover the criteria (mineral assemblages, textures, chemical partitioning, and phase equilibrium constraints) for distinguishing between magmatic, metamorphic, and metasomatic andalusite;
3. to evaluate the conditions and controls that promote the formation of andalusite in naturally occurring felsic igneous rocks.

If andalusite can have a primary magmatic origin, its occurrence places important constraints on the *T*–*P*–*X* conditions of magma crystallization.

Petrological framework

The positions of the water-saturated granite solidus and the andalusite–sillimanite stability field boundary in *T*–*P*–*X* space are critical to the origin of andalusite in felsic igneous rocks. At one extreme, simple synthetic systems involving the water-saturated haplogranite (Na_2O–K_2O–Al_2O_3–SiO_2–H_2O) solidus (Tuttle & Bowen, 1958; Holland & Powell, 2001) and the aluminosilicate stability fields (Holdaway, 1971; Holdaway & Mukhopadhyay, 1993) show no overlap between the stability fields of silicate melt and andalusite, precluding a primary magmatic origin for andalusite (Fig. 1a). Accordingly, andalusite in felsic igneous rocks must be xenocrystic, metasomatic, or the product of growth from a strongly undercooled melt. At the other extreme, simple synthetic systems involving the water-saturated peraluminous granite solidus (Abbott & Clarke, 1979; Holtz *et al*., 1992; Joyce & Voigt, 1994) and the aluminosilicate stability fields of Richardson *et al*. (1969) show substantial overlap, thereby permitting a primary magmatic origin for andalusite (Fig. 1b).

The position of the andalusite–sillimanite field boundary in *P*–*T* space has been investigated many times, but its precise location remains controversial (Kerrick, 1990; Pattison, 1992, 2001; Holdaway & Mukhopadhyay, 1993; Tinkham *et al*., 2001; Pattison *et al*., 2002; Cesare *et al*., 2003). Uncertainties in the position of the And = Sil field boundary arise, in part, from the strong dependence of the thermodynamic equilibrium conditions on the structural state of the material under investigation (Salje, 1986).

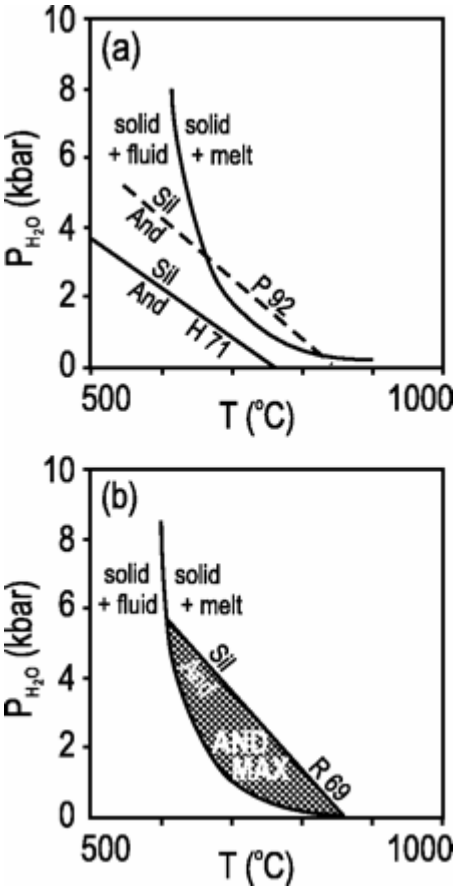


Fig. 1. Relationship between the granite solidus and the andalusite–sillimanite stability field boundary. (a) The combination of the haplogranite solidus (Tuttle & Bowen, 1958) and the And = Sil boundary of Holdaway (1971; H71) permits no overlap of the stability fields of andalusite and silicate melt, and precludes the stable crystallization of primary magmatic andalusite, whereas the combination of the haplogranite solidus and the And = Sil boundary of Pattison (1992; P92) permits the formation of primary magmatic andalusite. (b) The combination of the peraluminous granite solidus (Johannes & Holtz, 1996) and the And = Sil boundary of Richardson *et al.* (1969; R69) expands the stability field for andalusite + silicate melt (shaded area labelled 'AND MAX').

The position of the water-saturated granite solidus curve is sensitive to the presence of other components. In particular, excess Al_2O_3 lowers the solidus curve by *c*. 30°C (Fig. 1b), and creates a more favourable compositional environment in which to grow Al_2SiO_5 polymorphs (Abbott & Clarke, 1979; Clemens & Wall, 1981; Holtz *et al.*, 1992; Joyce & Voigt, 1994). Fluorine, lithium, and boron are other components that may have important roles in lowering the haplogranite solidus curve depending on their concentrations (Chorlton & Martin, 1978; London & Burt, 1982; Pichavant & Manning, 1984). Natural Ca-bearing plagioclase raises the haplogranite solidus curve by 10–20°C, depending on the amount of Ca in the system (Johannes, 1978).

Considerable discrepancy exists between the experimental studies of Richardson *et al.* (1969), who used fibrolitic sillimanite, and those of Holdaway (1971) who used prismatic sillimanite. According to Salje (1986), a 'transition field' between the polymorphs is more appropriate than a 'transition line'. Grambling & Williams (1985) and Kerrick (1990) suggested an effect of impurities (mainly Fe^{3+} and Mn^{3+}) on the stability relations of the Al_2SiO_5 polymorphs. Incorporation of Fe and Mn enlarges the stability field of

andalusite relative to that of sillimanite; however, Pattison (2001) argued that this effect is generally modest for natural Fe and Mn contents.

Owing to these difficulties in deciding between the different experimental calibrations, many investigators turned to natural parageneses to constrain the equilibrium (e.g. Greenwood, 1976; Vernon, 1982; Holland & Powell, 1985; Pattison, 1992; Pattison *et al*., 2002). Most of these studies placed the And = Sil equilibrium in positions intermediate between the Holdaway (1971) and Richardson *et al*. (1969) curves. Of particular significance to this investigation is that several studies of metapelitic And = Sil phase equilibria in low-pressure settings (i.e. those most relevant to the issue of andalusite + silicate melt stability) rejected the Holdaway (1971) And = Sil curve because it created too small an andalusite stability field to reconcile with a number of other phase equilibrium constraints (e.g. Vernon, 1982; Vernon *et al*., 1990; Pattison & Tracy, 1991; Pattison, 1992; Johnson & Vernon, 1995). Pattison (1992) provided an evaluation of the And = Sil equilibrium against a number of key phase equilibrium constraints that supported his calculated position about midway between the Holdaway (1971) and Richardson *et al*. (1969) positions. This position allows for an andalusite + haplogranite melt stability field below ~3 kbar, even without the need to invoke F-, B-, Li- or excess Al-bearing components in the melt (Fig. 1a), and it has found support in a number of recent papers (Spear *et al*., 1999; Tinkham *et al*., 2001; Cesare *et al*., 2003; Johnson *et al*., 2003; Larson & Sharp, 2003). In addition, the presence of melt inclusions in andalusite from volcanic rocks (Cesare *et al*., 2003), the presence of euhedral crystals of andalusite in some glassy felsic volcanic rocks (Pichavant *et al*., 1988), and the occurrence of euhedral andalusite crystals in granitic rocks and anatectic leucosomes (Clarke *et al*., 1976; Clemens & Wall, 1981; Vernon *et al*., 1990; Pattison, 1992) suggest an overlap of the stability fields of andalusite and silicate melt and a magmatic origin for the andalusite.

Methods

This project began as the result of an exchange of ideas about andalusite in granites on the Granite-Research Internet discussion group (granite-research@ac.dal.ca, now granite-research@lists.dal.ca). Subsequent to that discussion, Barrie Clarke and Michael Dorais tested some ideas with their own andalusite-bearing and andalusite-free granitoid samples, and then put out a request on the granite-research network for further contributions to expand the coverage. The result is a database of 111 felsic igneous rock samples, 108 of them containing andalusite, contributed by the authors of this paper. All authors have participated in the production of this paper through an exchange of text, tables, and figures on the Internet.

Most of the samples were submitted as hand specimens and prepared as thin sections by Gordon Brown at Dalhousie University. Petrographic observations of all samples were made by Barrie Clarke and Michael Dorais, and verified by the person submitting the samples. In this way, we have applied a uniform nomenclature to all samples. Bernardo Cesare examined all samples for melt

inclusions. Dan Kontak examined all samples for fluid inclusions. Where applicable, mineral abbreviations used in this paper are those of Kretz (1983).

PETROGRAPHIC OBSERVATIONS AND DISCUSSION

In a field and petrographic study, Hills (1938) noted that 'it is chiefly from those uncontaminated ... granites, pegmatites, and aplites...that what appears to be primary pyrogenetic andalusite has been recorded'. Hills' evidence included modal abundance, uniform distribution, large size and euhedral habit of andalusite, lack of oriented carbonaceous inclusions (chiastolite), absence of metasedimentary xenoliths, association with topaz and tourmaline in two-mica granites, and, for some, apparent lack of opportunity for the magmas to assimilate peraluminous wall-rock. To establish the igneous origin for a particular mineral requires matching a number of these, and other, inherently equivocal textural criteria, detailed below. If andalusite in a felsic igneous rock satisfies at least some of these criteria, an igneous origin for that andalusite is tenable.

Electronic Appendix Table A1 contains information about the samples, including source, location, environment of crystallization, and a literature reference (if any); electronic appendices may be downloaded from the *Journal of Petrology* website at http://petrology.oupjournals.org/.

Grain size

Dimensional compatibility of a mineral of unknown origin with other magmatic rock-forming minerals in the same sample could be used to argue a co-magmatic origin. The grain sizes of primary magmatic minerals in an igneous rock can, however, vary by orders of magnitude; therefore, any grain-size test is not particularly discriminating. Conversely, dimensional incompatibility may suggest, but does not necessarily demand a different origin. Any andalusite grains that are significantly smaller, or significantly larger, than the main rock-forming silicate minerals are potentially non-igneous. Figure 2 illustrates two samples (BBR-01 and CES-01) in which andalusite fails the grain-size test because the crystals are much larger than the other minerals in the rock. Many other samples contain andalusite grains that are considerably smaller than the main rock-forming minerals; although they also fail the grain-size test, they may still have an igneous origin.

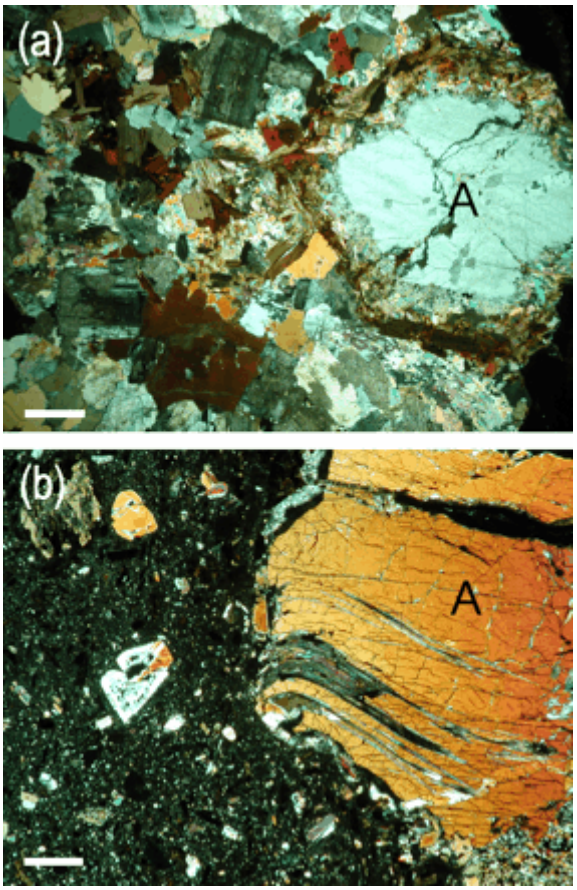


Fig. 2. Andalusite grain sizes. Photomicrographs illustrating andalusite grains that are significantly larger than the average grain size of the rock, suggesting that they may not have the same origin as the other minerals in these felsic igneous rocks. (a) Sample BBR-01 (granite; Oulad Ouslam Pluton, Morocco). (b) Sample CES-01 (dacite, Mazarrón, Spain). Scale bars represent 1 mm. A, andalusite.

Grain shape

Euhedral andalusite in a felsic igneous rock may indicate a former cotectic or peritectic relationship with a silicate melt phase; however, euhedral andalusite occurs both in igneous and metamorphic rocks, and thus idiomorphic grain shapes alone are not diagnostic. Some of the andalusites in volcanic samples, e.g. LON-01 (Fig. 3a), or aplites, e.g. WIL-01 (Fig. 3b), pass the grain-shape test as potentially primary magmatic phases. The andalusite in CLA-12 is skeletal (Fig. 3c), suggesting formation during a temperature or pressure quench. Many subhedral or anhedral andalusites in felsic igneous rocks have pink cores that are euhedral to subhedral (VIS-01, Fig. 3d), suggesting that those cores, at least, might be igneous.

Anhedral andalusite grain shapes may reflect late-stage grain interference during primary magmatic growth, the result of a reaction relationship of an andalusite of any origin with the silicate melt phase, an originally anhedral xenocrystic morphology, or an originally euhedral xenocrystic morphology out of equilibrium with the melt. Distinctly anhedral andalusite grains, apparently out of equilibrium with the felsic magma, include volcanic sample BAR-01 (Fig. 3e) and plutonic sample ROT-05 (Fig. 3f).



Fig. 3. Andalusite grain shapes. (a) Sample LON-01 (rhyolite obsidian clast, Macusani, Peru; US National Museum catalog no. 2143) shows two small euhedral to subhedral andalusite crystals in a predominantly glassy matrix. (b) Sample WIL-01 (aplitic granite; Velay Massif, France) contains euhedral andalusite. (c) Sample CLA-12 (aplite–pegmatite; South Mountain Batholith, Nova Scotia, Canada; section is slightly too thick) has elongate–skeletal andalusite grain shapes suggesting crystallization by quenching. (d) Sample VIS-01 (granite; Makalu north side, Tibet) has andalusite with an overall anhedral grain shape, but with a more euhedral pink core. (e) Sample BAR-01 (rhyolite; Lipari, Italy) is a volcanic rock with anhedral andalusite. (f) Sample ROT-05 (granite; Telve, Cima d'Asta pluton, southern Alps, Italy) contains anhedral andalusite that exhibits deformation twinning in crossed polars (not shown). Scale bars represent 1 mm. A, andalusite.

State of aggregation

Andalusite in felsic igneous rocks may occur as single grains (Figs 3a, b, d–f; 4a–d), isolated from other andalusite grains by more common rock-forming minerals. It may also occur as clusters of small grains. In some clusters, the individual andalusite grains have random orientations relative to one another (Fig. 5a–d). Why should a modally scarce mineral cluster? Either the individual andalusites crystallized elsewhere and were brought to that location by some physical process such as synneusis or settling, or they represent the sites of advanced digestion of pelitic xenoliths, or they nucleated and grew at that position in the sample. These common clusters of randomly oriented grains of andalusite may have genetic significance.

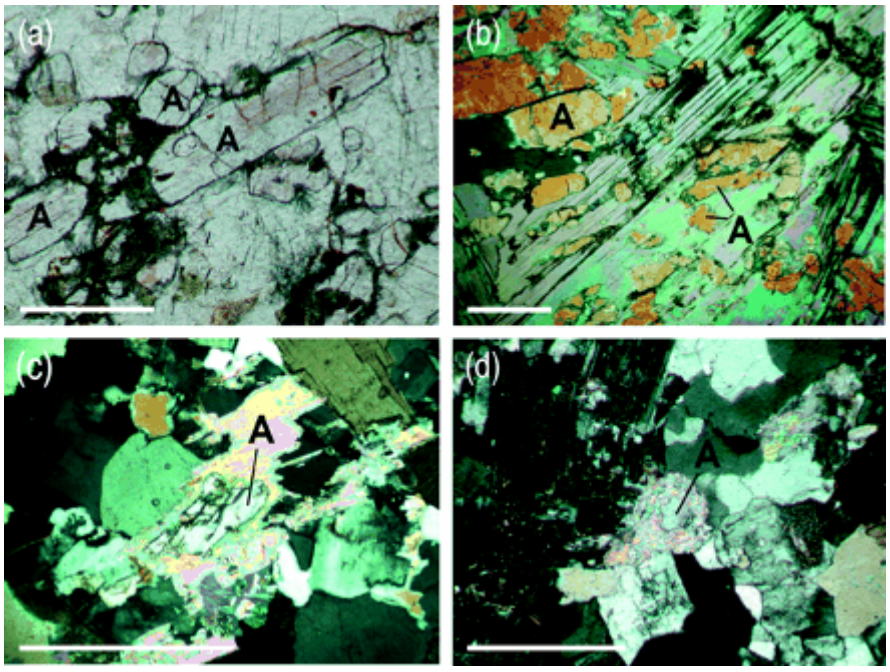


Fig. 4. Single grains of andalusite. (a) Sample CLR-01 (migmatite; Mt. Stafford, Arunta Block, Australia) with subhedral andalusite in a migmatite leucosome (textural type S1). (b) Sample TOS-05 (pegmatite; Velasco Batholith, Argentina) shows a single optically continuous andalusite grain enclosed in single grain of muscovite (textural type S2). (c) Sample ROT-02 (granite; Cotronei, Sila Batholith, Calabria, southern Italy) showing a subhedral andalusite enclosed in a single crystal of muscovite (textural type S2). (d) Sample UGI-04 (granite; Plasencia granite, west Central Iberian Massif, Spain) showing an anhedral andalusite with a polycrystalline rim of muscovite (textural type S3). Classification of textural types S1, S2, and S3 is given in Fig. 6. Scale bars represent 1 mm. A, andalusite.

In other clusters, the individual andalusite grains are in optical and crystallographic continuity (e.g. Figs 3c and 4b). If in crystallographic alignment, the andalusite grains either grew as a spray of quench crystals (Figs 3c and 5b), or the clustering may only be apparent, as in the cases of many optically continuous andalusite grains embedded in muscovite (Fig. 4b). In cases such as the latter, a single grain of andalusite was irregularly replaced by muscovite, yielding an apparent ‘cluster’ of anhedral, but crystallographically aligned, andalusite in muscovite.

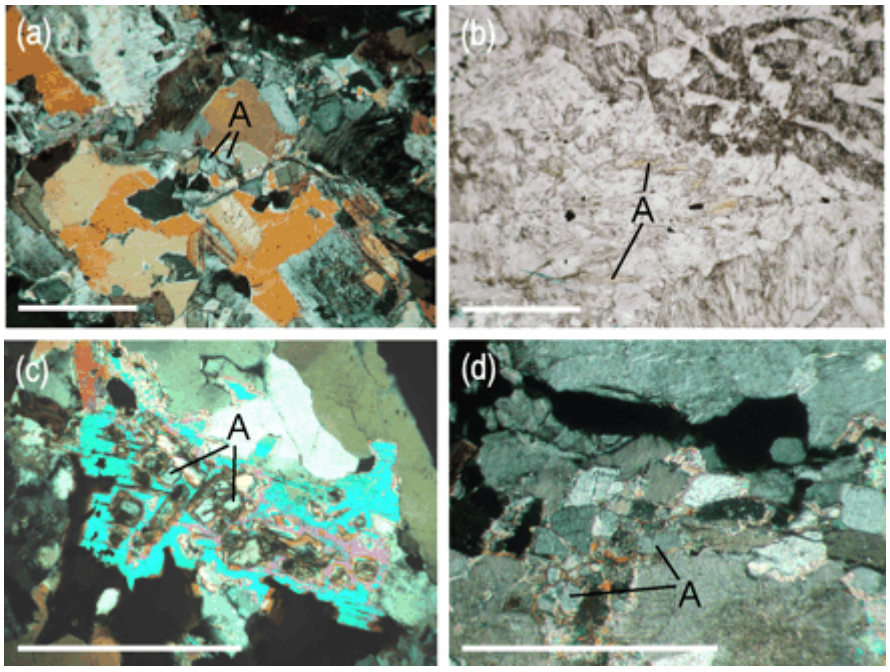


Fig. 5. Clusters of andalusite grains. (a) Sample ROT-04 (granite; Rasna quarry, Telc, southwestern Moravia, Czech Republic) showing a small cluster of anhedral andalusite crystals in quartz (textural type C1). (b) Sample ELB-01 (aplite; Beni Bousera, Morocco) showing a sub-parallel cluster of andalusite grains in an aplite (textural type C1). (c) Sample ROB-02 (granite; South Bohemian Pluton, Austria) shows a cluster of randomly oriented andalusites in a single crystal of muscovite (textural type C2). (d) Sample VIL-02 (granite; Peña-Hombre Pluton, Spain) shows a cluster of anhedral andalusite grains in a polycrystalline aggregate of muscovite (textural type C3). Classification of textural types C1, C2, and C3 is given in Fig. 6. Scale bars represent 1 mm.

Textural relationship with muscovite

Many andalusite grains in felsic igneous rocks have mantles of muscovite, and these muscovite rims may consist of a single crystal or a polycrystalline aggregate. Figure 6 combines the state of aggregation of andalusite grains (above), and the common association of andalusite with muscovite, to establish a six-fold textural classification of andalusite. In some cases, more than one class of andalusite can occur in the same rock (e.g. sample GOT-02 contains andalusite textural types S1, C1, and C2).

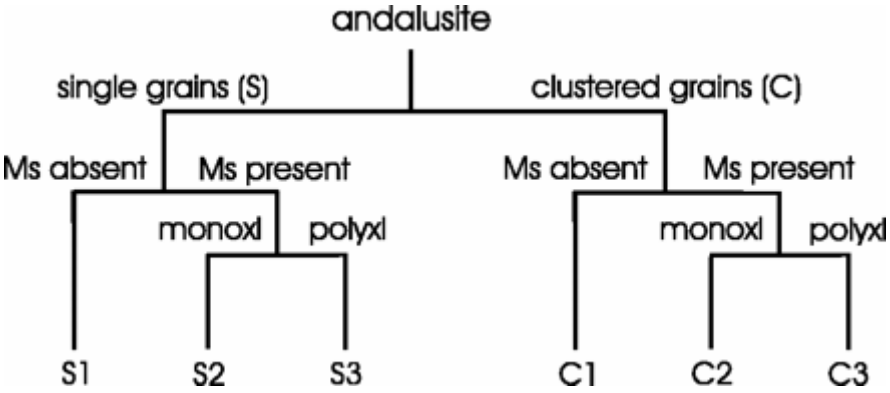


Fig. 6. Textural classification of andalusite in felsic igneous rocks. Three textural parameters (the occurrence of andalusite either as single grains or as clusters of grains, the occurrence of andalusite with or without muscovite, and if with muscovite, whether that muscovite consists of a single grain or an aggregate of grains) produce the following six textural categories: S1, single andalusite grains, no muscovite; S2, single andalusite grains, monocrystalline muscovite overgrowth or reaction rim; S3, single andalusite grains, polycrystalline muscovite overgrowth or reaction rim; C1, clustered andalusite grains, no muscovite; C2, clustered andalusite grains, monocrystalline muscovite overgrowth or reaction rim; C3, clustered andalusite grains, polycrystalline muscovite overgrowth or reaction rim. Textural types S1 and C1 can occur as discrete grains, or as inclusions in other grains such as plagioclase or quartz.

In the Macusani rhyolites, muscovite and andalusite coexist throughout the entire volcanic field (Pichavant *et al.*, 1988). No textural evidence exists for replacement of one phase by the other, but the modal proportions of andalusite and muscovite are negatively correlated, suggesting that, during the main crystallization stage of the Macusani magmas, the reaction Ms + Qtz = And + San (in presence of melt) controls the modal proportions of andalusite and muscovite. This reaction depends on P, T, and a_{H2O}, implying that the mineral assemblage characteristic of the main crystallization stage of the Macusani magmas (Qtz, San, Plag, Ms, And, ± Bt) could have crystallized over a range of P, T and f_{H2O} conditions. However, the F content of muscovite is also an important controlling factor in this reaction. For a given a_{H2O}, elevated f_{HF} would drive the reaction to the left (consuming andalusite, producing muscovite). Muscovite crystallization at the expense of andalusite does not necessarily imply high a_{H2O} (it could be lower T, higher P, or higher f_{HF}). The inverse correlation between the modal proportions of Ms and And in the Macusani volcanics also occurs in peraluminous granites from the Bohemian Massif (samples ROT-03,04; D'Amico *et al.*, 1982–1983*a*, 1982–1983*b*).

Muscovite overgrowths on andalusite in plutonic rocks may obscure a possible original euhedral shape (ROT-02, Fig. 4c), and thereby complicate any determination of the origin of the andalusite. Because muscovite can have primary magmatic or secondary hydrothermal origins, with much the same texture (Miller *et al.*, 1981; Zen, 1988), interpretation of this textural relationship between andalusite and muscovite is difficult. One reason for little or no bulk chemical compositional difference between some andalusite-bearing two-mica granitoids and andalusite-free two-mica granitoids is just a question of

how completely the andalusite is replaced (effectively under magmatic conditions by primary muscovite, less effectively under subsolidus conditions by secondary muscovite). Whether andalusite is preserved in plutonic rocks depends on its survival under conditions of slow cooling, allowing magmatic peritectic relations of the type

$$\mathrm{L} + \mathrm{And} + \mathrm{Other\ Phases} \rightarrow \mathrm{L} + \mathrm{Ms} + \mathrm{Other\ Phases}$$

(where L is melt), or subsolidus reactions such as

$$\mathrm{And} + \mathrm{Kfs} + (\mathrm{H_2O})_{\mathrm{v}} \rightarrow \mathrm{Ms} + \mathrm{Qtz}$$

to eliminate the early formed andalusite. Addition of water to the left sides of these equations converts 'dry' andalusite-bearing granitoids to 'wet' muscovite-bearing, and normally two-mica, granitoids; in other words, they are compositional equivalents except for the amount of water (Zen, 1989). Kinetically, a high-temperature, melt + fluid, condition may favour the formation of coarse-grained single muscovite crystals, whereas a subsolidus low-temperature, fluid-only, condition may favour the formation of some fine-grained polycrystalline muscovite aggregates.

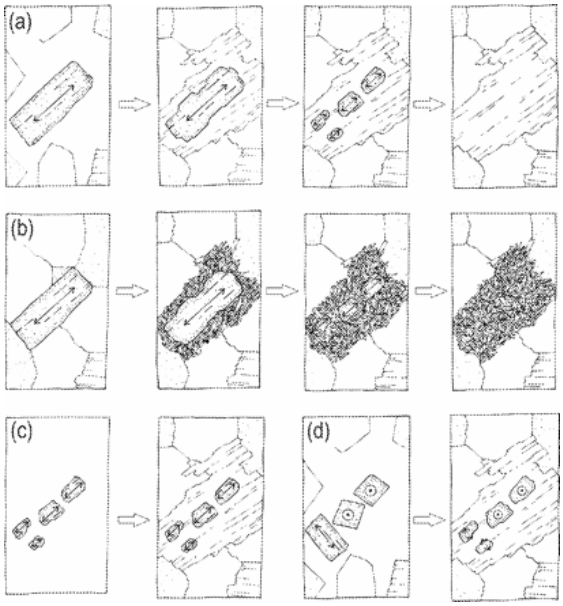


Fig. 7. Development of several possible textural relationships between andalusite and muscovite (arrows represent the crystallographic *c*-axis of andalusite). Different processes can have similar end-points. (a) Single grain of magmatic muscovite overgrows a single grain of magmatic andalusite. Suprasolidus or subsolidus muscovite continues to grow to the ultimate elimination of andalusite. No textural evidence for the former existence of andalusite remains. (b) Subsolidus replacement of a single grain of andalusite to produce a polycrystalline muscovite pseudomorph. (c) Quenched skeletal andalusite overgrown by magmatic muscovite resulting in an apparent cluster, but the 'grains' are in optical continuity. (d) Optically discontinuous cluster overgrown by magmatic muscovite.

Figure 7 illustrates four of the many types of textural relations between andalusite and muscovite. The original andalusite may be a single grain or a cluster, the muscovite rim may be magmatic or subsolidus hydrothermal, and the And →Ms reaction may be incomplete or complete. In the last case, the andalusite is completely consumed in the reaction, leaving little or no evidence of its former existence.

Inclusion relationships

Mineral inclusions

If andalusite occurs as inclusions in igneous minerals such as feldspar and quartz (e.g. REN-03, UGI-06), little can be deduced about its origin; however, andalusite rarely occurs as inclusions in any phase other than muscovite. If andalusite itself contains inclusions of magmatic minerals, the sizes, shapes, abundances, and compositions of those inclusions may help to determine the origin of the host andalusite. If an andalusite contains carbonaceous material defining the chiastolite cross (e.g. BBR-01, Fig. 2a), a metamorphic origin is probable. Some chiastolite-like andalusite may also form by peritectic melting reactions in graphitic schists where inclusion of graphite particles may take place behind advancing crystal faces, but at the same time the andalusite should also trap melt inclusions (Cesare & Gómez-Pugnaire, 2001). Few of the andalusites that we believe are igneous on other grounds contain any mineral inclusions, and thus the mineral inclusion criterion is not particularly useful.

Melt inclusions

Melt inclusions in andalusite attest to its growth in the presence of melt (Cesare *et al.*, 2003). Glass inclusions are easy to recognize in andalusite from felsic volcanic rocks, such as those from Lipari (BAR-01), Mazarrón (CES-01,02) (Cesare & Gómez-Pugnaire, 2001; Cesare *et al.*, 2002, 2003), and Macusani (Pichavant *et al.*, 1988; Fig. 8). In slowly cooled plutonic rocks or migmatites, any melt inclusions trapped in andalusite will have crystallized as polyphase aggregates of quartz, feldspars, and micas, a useful criterion to infer an igneous origin for andalusite. Polyphase inclusions in andalusite crystals of samples CLA-01,05,11,12,13, CLR-02, GOM-03, RIC-03, and TOS-06 provide additional support for their coexistence with a felsic silicate melt.

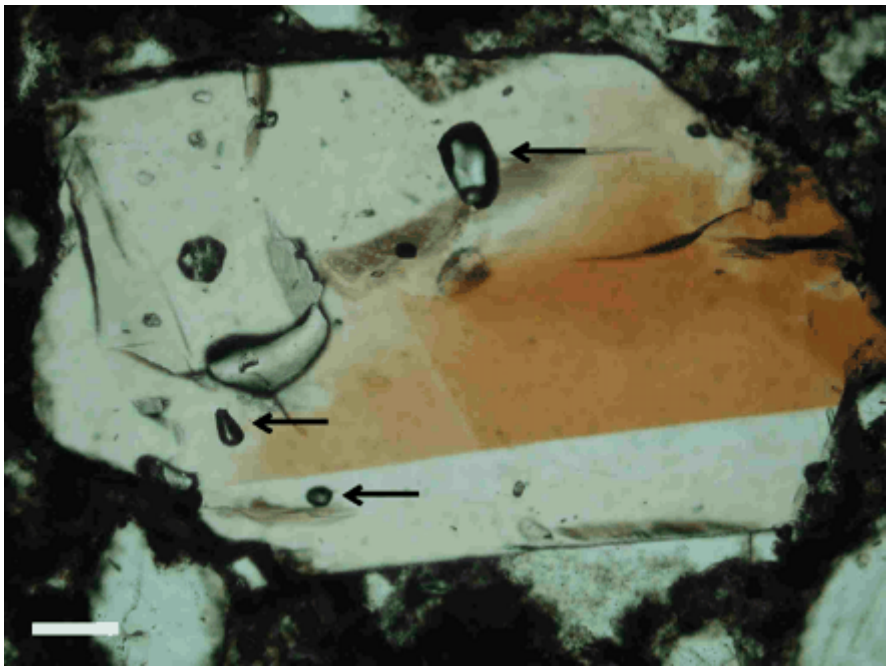


Fig. 8. Melt inclusions in andalusite. Volcanic sample PIC-01 (rhyolite; Macusani, Peru) showing conspicuous melt inclusions. Also to be noted is the sharp straight contact between the pleochroic core and the colourless rim of the andalusite. Scale bar represents 0·1 mm.

Fluid inclusions

Examination of all our andalusite samples for fluid inclusions yielded negative results. Either there was no fluid in equilibrium with the andalusite as it grew (unlikely in the cases of pegmatites), or the surface properties of andalusite are such that it is not readily 'wetted' by fluids.

Summary of textural observations

Of the several possible textural tests for the origin of andalusite in felsic igneous rocks, no single criterion (grain size, grain shape, clustering, textural relations with muscovite, inclusion relations) is necessarily diagnostic of the origin of andalusite. The agreement of two or more of these textural and chemical criteria constitutes a stronger collective case. For example, a euhedral, grain-size compatible, andalusite with melt inclusions occurring in a volcanic rock is almost certainly magmatic, whereas a large anhedral andalusite with a chiastolite cross and a reaction rim is probably xenocrystic. Also, we note that there is no *a priori* textural reason why a felsic igneous rock cannot contain more than one genetic type of andalusite (e.g. magmatic and xenocrystic).

CHEMICAL COMPOSITION OF ANDALUSITE IN FELSIC IGNEOUS ROCKS

In this section, we examine the chemical composition of andalusite, the nature of any chemical zoning, and the chemical compositions of coexisting micas and apatite to search for criteria that might provide information about the origin of andalusite in felsic igneous rocks. Electronic Appendix Tables A2–A5 contain compositional data for average biotite, muscovite, andalusite, and apatite, respectively, in the samples we have studied. Not all samples contain all four minerals, and even if they do, we do not necessarily have analyses for all four phases in each rock.

Chemical composition

If a mineral exhibits a wide range of chemical substitutions that reflect its conditions of formation [e.g. Ti in muscovite (Miller *et al.*, 1981)], then the origin of that mineral may be determined from its chemical composition alone. In stoichiometric andalusite (Al_2SiO_5), half the Al cations reside in octahedral sites, and the other half reside in five-coordinated polyhedra, whereas all the Si cations occupy tetrahedral sites. Such simple chemistry and relatively simple structure provide limited opportunity for chemical substitution (Deer *et al.*, 1982). Electronic Appendix Table A4 shows that the studied andalusites from felsic igneous rocks have transition-element compositions with the following ranges: FeO_T (measured as Fe, reported as FeO) 0·03–1·70%, MnO 0·00–0·09%, and TiO_2 0·00–0·36%. Without a comparable database of andalusite compositions from metamorphic rocks, little can be said about the existence of chemical discriminants to determine the origin of the andalusite. Trace elements might prove to be more useful than major elements.

Chemical zoning

Optically zoned andalusite is common in metamorphic, hydrothermal, and magmatic environments [e.g. review by Kerrick (1990)]. Andalusites from the studied felsic igneous rocks show four types of zoning, as follows.

1. *Concentric zoning*. Concentric zoning consists of a sharp to gradational variation in the mole fraction of transition-element content (hereafter referred to simply as TE content) from core to rim, with some boundaries subparallel to the external morphology of the crystal (Fig. 9a). However, the cores of such grains may be highly irregular in shape, showing convolute–lobate and/or irregularly stepped boundaries (Fig. 9b).
2. *Sector zoning*. Sector zoning is characterized by higher TE contents parallel to {001}, {100}, and {010} (Hollister & Bence, 1967). Regular steps in some of the concentric zone boundaries may be sector zone boundaries. The most striking example is from sample ERD-01, which shows sharp subhedral sector zoning (Fig. 9c); the steps in the zoning of andalusite VIL-05 (Fig. 9b) may also represent preferential sector growth.

3. *Oscillatory zoning*. Oscillatory zoning is characterized by alternating high-TE and low-TE, continuous to discontinuous, growth shells (Fig. 9d and e). Most boundaries between the growth zones are either rounded or irregularly stepped.
4. *Patchy zoning*. In contrast to sector zoning above, patchy zoning shows neither sharp nor obviously crystallographically controlled boundaries (Fig. 4a).

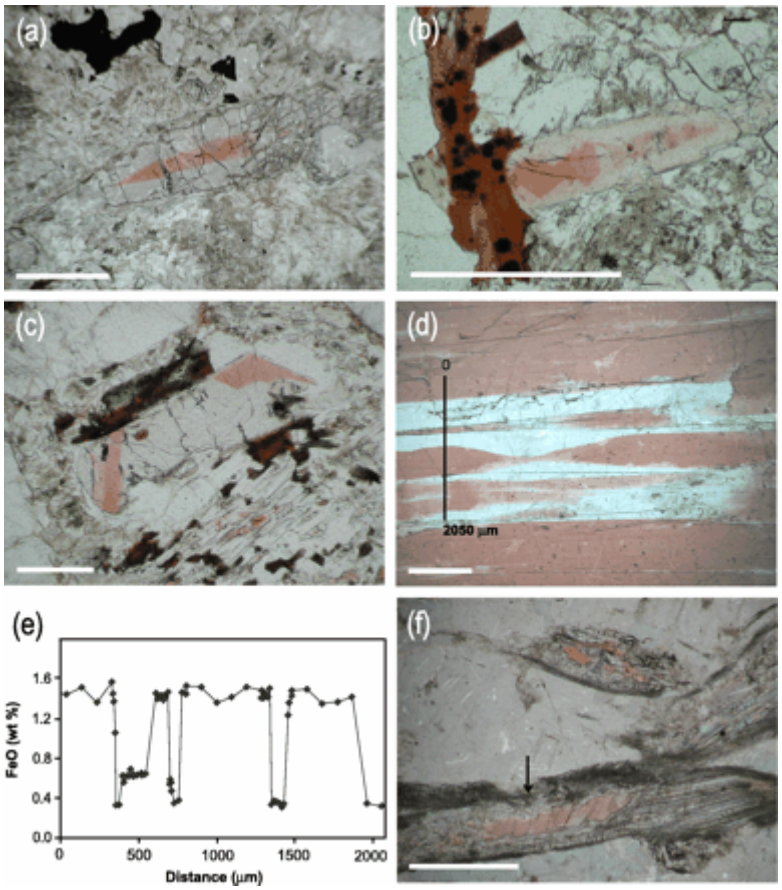


Fig. 9. Chemical zoning in andalusite. (a) Sample CLA-05 [migmatite(?); South Mountain Batholith, Nova Scotia, Canada] shows normal–concentric zoning, with one sharp zone boundary and one gradational zone boundary, mimicking the external morphology of the crystal. (b) Sample VIL-05 (granite; Berrocoto Pluton, Spain) shows irregular normal–concentric zoning with straight sharp and curved gradational zone boundaries. (c) Sample ERD-01 (aplite–pegmatite; South Mountain Batholith, Nova Scotia, Canada) shows well-developed sector zoning. (d) Sample GOM-12 (pegmatite; Pacos de Ferreira, Portugal) shows irregular, sharp to gradational, oscillatory zoning. (e) Line scan for iron along profile in (d). The pink zones correspond to high iron contents. (f) Sample WHI-01 (granite; Nigde Massif, Turkey) shows preservation of original zoning in andalusite subjected to sillimanite-grade metamorphism (arrow). Scale bars represent 1 mm.

Once formed, such andalusite zoning patterns appear to be robust, as indicated by samples WHI-01 (Fig. 9f) and NEV-04 (not shown) in which the pink TE-rich andalusite cores have survived high-temperature sillimanite-grade metamorphism, but the outer parts of the colourless rims have inverted to sillimanite.

Although the different types of zoning in andalusite are well known, little is understood about their origins and their potential for revealing diagnostic information about *T–P–X* crystallization environments. Hydrothermal andalusite commonly shows concentric zoning (high-TE core, low-TE rim) or sector zoning (Cesare, 1994; Whitney & Dilek, 2000), whereas metamorphic andalusite commonly shows gradational patchy zoning, and may also exhibit concentric zoning (Yokoi, 1983; Shiba, 1988; Cesare, 1994), or sector zoning (Grambling & Williams, 1985). If distinctions between environments of crystallization exist, they are not yet well defined. Nevertheless, zoning patterns may help to exclude a certain origin for a grain in question (e.g. oscillatory zoning is unlikely for metamorphic andalusite, but likely for hydrothermal or magmatic andalusite). Several features of zoned andalusites are, at least, consistent with a magmatic origin (e.g. sharp compositional zone boundaries, oscillatory zones, possible quench phenomena with preferential sector growth). Unfortunately, we do not yet have sufficient textural and chemical information about zoned andalusites in veins and metamorphic rocks to be able to distinguish clearly between one environment of crystallization and another, and what, if any, characteristics of zoning are unique to magmatic andalusites.

Chemical equilibrium with other minerals

For minerals showing extensive mutual solid solution, systematic disposition of tie lines between coexisting phases is an indication of an equilibrium relationship. In this section, we consider whether the compositions of biotite, muscovite, and apatite coexisting with andalusite are consistent with their being an equilibrium assemblage. If they are in chemical equilibrium with each other and magmatic in origin, and if they are also in chemical equilibrium with andalusite, then the andalusite should also be magmatic.

Biotite

Figure 10a is a trioctahedral mica plot showing the average biotite compositions in all the studied samples. Given the global distribution of the samples, the consistency of the Al^{iv} [mean 2·68 ± 0·07 atoms per formula unit (a.p.f.u.)] in the biotites is remarkable, suggesting that the biotites have had their alumina contents fixed by equilibrating with some Al-rich phase (e.g. andalusite), probably under conditions of restricted temperature and pressure. Although a magma containing abundant andalusite and biotite xenocrysts might also attain this equilibrium, the simplest interpretation is that the biotite and andalusite are both primary magmatic in origin.

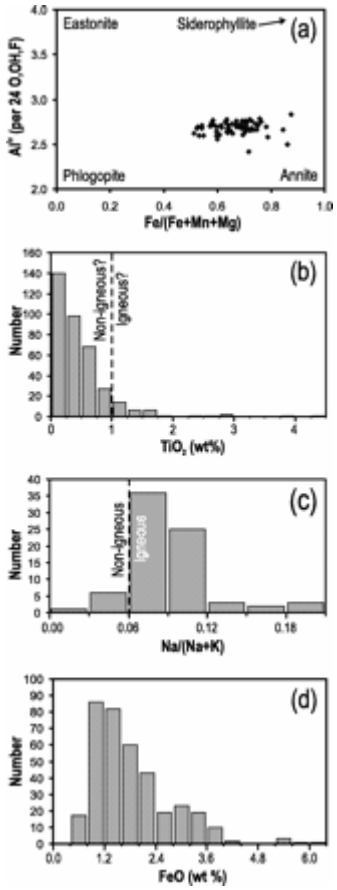


Fig. 10. Compositions of coexisting micas. (a) Biotite compositions in the system phlogopite–annite–eastonite–siderophyllite. Despite the genetically unrelated nature of the sample set, biotite compositions from the studied suite of andalusite-bearing rocks have tightly constrained Al^{iv} ≈2·68 ± 0·07 a.p.f.u. (b) TiO_2 contents of all analyzed muscovites in the sample set. The distribution is strongly skewed to low TiO_2 contents (<1%). (c) Na/(Na + K) values showing the boundary between non-igneous and igneous muscovites (Monier *et al.*, 1984). (d) FeO contents of all analyzed muscovites.

Muscovite

Figure 10b and c shows the TiO_2 and Na/(Na + K) distributions in all analyzed muscovite grains. According to the chemical criteria of Miller *et al.* (1981), very few of these muscovites have TiO_2 >1%, consistent with a primary magmatic origin; however, if a highly evolved magma has a very low TiO_2 content, so presumably, will its primary magmatic muscovite. According to their Na/(Na + K) ratios, however, these muscovites are predominantly magmatic (Monier *et al.*, 1984). Figure 10d shows the variable, but non-diagnostic, range of FeO concentrations in the muscovites coexisting with andalusite.

For the composition of muscovite to be more useful, we need a detailed study of muscovite associated with andalusite versus the rest of the muscovite in the rock. Furthermore, we need to determine if there is any chemical difference between the monocrystalline muscovite rims on andalusite (magmatic?) and the polycrystalline muscovite rims on andalusite (hydrothermal? quenched?).

Biotite + *muscovite*

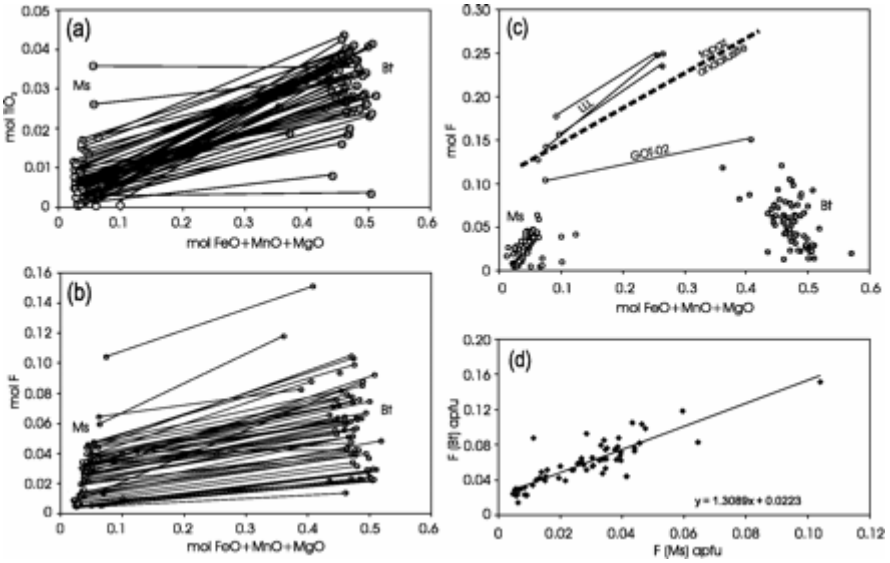


Fig. 11. Average muscovite and biotite compositions. Tie lines join coexisting pairs. (a) Molecular (FeO + MnO + MgO) vs TiO_2. (b) Molecular (FeO + MnO + MgO) vs F. In both plots, most mica compositions appear to represent equilibrium pairs, and the simplest interpretation is that they are magmatic phases in equilibrium with (magmatic) andalusite. (c) The andalusite-bearing sample with the highest F content in coexisting micas is GOT-02 (high fluorine, high phosphorus, granite; Satzung, Erzgebirge, Germany). Also plotted are micas coexisting with primary magmatic topaz in the Lake Lewis leucogranite in the South Mountain Batholith (LLL; Clarke & Bogutyn, 2003). The dashed line is the inferred upper limit for fluorine in micas of andalusite-bearing granites. (d) Partitioning of fluorine between coexisting micas in the sample set. The calculated partition coefficients are generally consistent with experimentally determined values (Icenhower & London, 1995).

In general, andalusite-bearing plutonic rocks contain biotite and muscovite with high alumina contents; however, this criterion alone does not necessarily separate igneous from metamorphic micas. Figure 11a shows TiO_2 contents for averages of all analyzed mica pairs.

Figure 11b shows mean fluorine concentrations for the same coexisting micas. Of note is the wide range of F contents in the micas in these andalusite-bearing rocks, and the generally regular disposition of tie lines suggesting equilibrium compositions. Tie lines with distinctively steeper or shallower slopes suggest that the composition of at least one mica in the assemblage has changed, and that some degree of subsolidus re-equilibration of F between coexisting micas may have taken place. In such cases, $D_F^{Bt/Ms}$ increases with subsolidus cooling because muscovite re-equilibrates more readily than biotite (Ferrow *et al.*, 1990). Such disequilibrium between the micas may also raise questions about the origin of the coexisting andalusite.

Samples with F_{Bt}/F_{Ms} <1·5 are VIL-14 and WOO-01, which appear to be otherwise unremarkable. Samples with F_{Bt}/F_{Ms} >3·8 are JAM-01, JAM-02, RIC-01, RIC-02, RIC-03, RIC-05, RIC-06, and NEV-02. Significantly, seven of these samples are migmatites with low F_{Bt} contents, and the other sample is a

pegmatite (NEV-02). Sample CLA-05 has the lowest F contents in its coexisting micas; in this respect, its similarity to the migmatites suggests that it may also have an early anatectic origin. The mean of all samples with average F_{Bt}/F_{Ms} >1·4 and <3·8 is 2·27 ± 0·59 (n = 31). In two samples with crossing tie lines (NEV-03, NEV-05), andalusite occurs in clusters with biotite-rich xenolithic material and texturally (but not chemically) secondary muscovite. Because all of these samples contain andalusite, high F is, apparently, not a precondition for the occurrence of andalusite in felsic igneous rocks.

If all the analyzed samples had come from one differentiating pluton, such a regular disposition of tie lines might be expected; however, given that the samples come from more than 40 localities of different types, the regularity of the tie lines in Fig. 11a and b suggests an important repetition of *T–P–X* conditions in andalusite-bearing peraluminous felsic igneous rocks through space and time. As a first-order approximation, we consider the bundles of roughly parallel tie lines (Fig. 11a and b) and the samples with Ti and F partitioning between coexisting micas similar to those determined experimentally (Icenhower & London, 1995), as magmatic micas. Figure 11c is similar to Fig. 11b, except that the vertical axis is expanded and most of the tie lines have been removed. Additional plotted samples are from the topaz-bearing two-mica Lake Lewis leucogranite in the South Mountain Batholith (Clarke & Bogutyn, 2003). Sample GOT-02 is the most fluorine-rich, andalusite-bearing, topaz-absent, sample from our database, and it helps to constrain the position of the andalusite–topaz boundary in this system.

Figure 11d shows the systematic partitioning of F between biotite and muscovite expressed by the equation $F_{Bt} = 1{\cdot}31\ F_{Ms} + 0{\cdot}02$. This empirical relationship is reasonably consistent with other data from coexisting micas in granites (F_{Bt}/F_{Ms} = 1·8 ± 0·5; Neves, 1997), and on coexisting micas in peraluminous experimental systems (F_{Bt}/F_{Ms} = 1·22–1·55; Icenhower & London, 1995).

Biotite + muscovite + apatite

The magmatic origin of apatite is normally not in question. Apatite should, therefore, exhibit systematic partition relationships for fluorine with the two other magmatic F-bearing phases, i.e. biotite and muscovite, if they are all in equilibrium. Figure 12a and b shows the complex relationship F_{Ap}/F_{Ms} vs F_{Ap}/F_{Bt}, contoured for F_{Bt} and F_{Ms}, respectively. In general, the array of points defines a curved trend, and in both plots the fluorine concentrations are highest in those micas with the lowest F_{Ap}/F_{Mica} values. This relationship appears to be the result of relatively constant fluorine concentrations in the apatites. The ratio of F_{max}/F_{min} in each of the phases in our entire sample set is 1·4 for apatite, 8·8 for biotite, and 27·7 for muscovite. Furthermore, samples with low bulk-rock fluorine contents, as proxied by the F_{Bt} values, have the fluorine strongly partitioned into the apatites (as before, many of these samples are migmatitic leucosomes). If the bulk-rock fluorine contents are high, F strongly partitions into the micas. The systematic partitioning of F between apatite and

the micas suggests equilibrium conditions. If the apatite is magmatic, then probably so should be the micas.

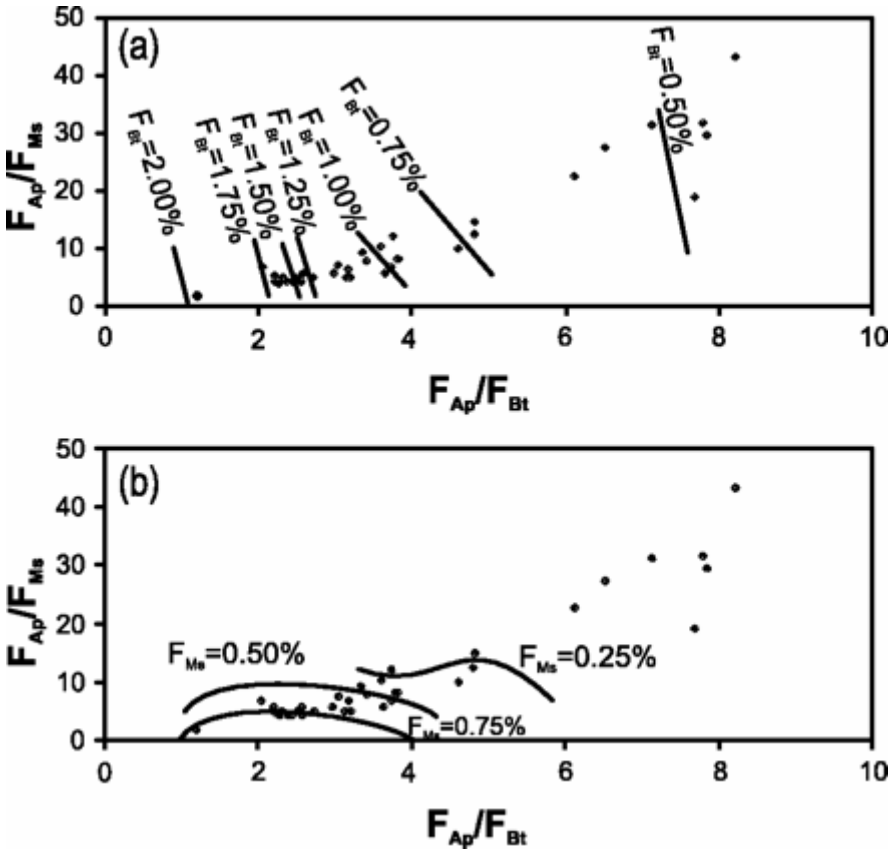


Fig. 12. Fluorine in coexisting apatite, biotite, and muscovite. (a) F_{Ap}/F_{Ms} vs F_{Ap}/F_{Bt} with F_{Bt} contours. The systematic distribution of F_{Bt} contours suggests equilibrium among the three phases. High F_{Ap}/F_{Ms} and F_{Ap}/F_{Bt} ratios correlate with low bulk fluorine contents as monitored by F in biotite. (b) F_{Ap}/F_{Ms}–F_{Ap}/F_{Bt} with F_{Ms} contours. Again, high F_{Ap}/F_{Ms} and F_{Ap}/F_{Bt} ratios correlate with low bulk fluorine contents, and the systematic distribution of contours suggests equilibrium among these three phases.

Sillimanite

The broad overlap of stability fields for sillimanite and felsic melt means that, in contrast to andalusite, an igneous origin for sillimanite in felsic igneous rocks is not a petrogenetic problem. Sillimanite can occur as the only aluminosilicate phase (D'Amico *et al*., 1982–83*a*, 1982–83*b*; Pichavant *et al*., 1988), or it can occur with andalusite (Barker, 1987; Pichavant *et al*., 1988; Messina *et al*., 1991; Rottura *et al*., 1993; Cesare *et al*., 2002; Visonà & Lombardo, 2002). Our sample set was assembled solely on the basis of the presence of andalusite; the additional occurrence of sillimanite in any sample was incidental. Our database is not sufficiently comprehensive to draw any general conclusions about the coexistence of andalusite and sillimanite in felsic igneous rocks.

Summary of chemical criteria

We have considered three chemical tests for the origin of andalusite in felsic igneous rocks. The chemical composition of andalusite itself provides little information about its origin. The nature of chemical zoning may have greater potential, but it first requires a more detailed examination of chemical zoning patterns in andalusites from metamorphic rocks and hydrothermal veins. The chemical-equilibrium-with-other-phases test is the most quantitative and most objective. Systematic partitioning of Ti and F between coexisting biotite, muscovite, and apatite in our sample set suggests that they are in equilibrium and are almost certainly magmatic phases. That the magmatic biotite also has its Al^{iv} controlled by equilibrium with andalusite is, we believe, the most compelling chemical argument in favour of a magmatic origin for the andalusite; however, this view does not entirely preclude the equilibration of xenocrystic biotite and andalusite at magmatic temperatures. We note again that there is no *a priori* chemical reason why a felsic igneous rock may not contain more than one genetic type of andalusite (e.g. magmatic and xenocrystic).

GENETIC TYPES OF ANDALUSITE IN FELSIC IGNEOUS ROCKS

Theoretically, andalusites in felsic igneous rocks can fall into three main genetic categories detailed below.

Type 1 Metamorphic (melt phase not involved in the formation of andalusite)

Type 1a Metamorphic–in situ prograde

Barrera *et al.* (1985) and Zaleski (1985) described the effects of contact metamorphism in granites where andalusite formed as euhedral to subhedral prisms replacing original biotite. None of the andalusite in our samples appears to have formed *in situ* by thermal metamorphism of a felsic igneous rock. In the sample most obviously affected by thermal metamorphism (WHI-01; Fig. 9g), pre-existing andalusite has been partially converted to sillimanite.

Type 1b Metamorphic–retrograde inversion of sillimanite of various origins

If sillimanite of any origin (magmatic, metamorphic) were present in a granite magma, it could undergo inversion to andalusite above or below the granite solidus, possibly resulting in andalusite pseudomorphs after the sillimanite. Barker (1987) has argued that, on the basis of size and shape of the andalusites in sample BAR-01 from Lipari, they have inverted from xenocrystic sillimanite. Otherwise, none of our andalusite appears to have formed by inversion from sillimanite.

Type 1c Metamorphic–xenocrystic derived from local peraluminous country rocks

Andalusite crystals may be released from disaggregating, contact-metamorphosed, metapelites into a silicate melt and, in general, such xenocrystic grains would be out of chemical equilibrium with that melt. These xenocrysts may be anhedral and contain many mineral inclusions, including carbonaceous material. Their subsequent history in the magma then depends on the degree to which they are out of equilibrium with the silicate melt, and on the kinetics of the new environment. Xenocrystic andalusite may disappear rapidly in a high-temperature, well-mixed, relatively fluid metaluminous melt, or in a peraluminous melt undersaturated in Al_2SiO_5, survive largely unmodified in a near-solidus, static, viscous peraluminous melt, or even develop magmatic overgrowths in a highly peraluminous melt. Xenocrysts in an advanced state of dissolution, especially if mantled by late muscovite, would be difficult to distinguish from anhedral magmatic grains.

Bouloton *et al*. (1991) and Bouloton (1992) described xenocrystic andalusite in Hercynian granites from Morocco where chiastolite-type crystals, up to 5 cm long, occur. Samples BBR-01 (Fig. 2a) and BBR-02 are from the same pluton. These large andalusites fail the grain-size test as magmatic, and they have significant reaction rims indicating disequilibrium with the melt. Also, samples NEV-03 to NEV-05 contain ovoid polymineralic aggregates of biotite, andalusite, and muscovite, with or without sillimanite, showing a symplectitic relationship. These aggregates only occur close (~300 m) to the contact with younger porphyritic biotite granites, and they appear to be foreign to their granite host.

López Ruiz & Rodríguez Badiola (1980) interpreted the origin of andalusite in some high-K dacites as xenocrystic because typical anhedral andalusite grains are surrounded by plagioclase and spinel reaction rims. Such andalusite grains may also contain inclusions, including the chiastolite cross, as well as textural evidence of disequilibrium (e.g. corrosion). Alternatively, because some of these andalusites also contain melt inclusions, Cesare *et al*. (2003) regarded them as Type 1d or 2a (below).

Type 1d Metamorphic–original constituent of source rocks (restitic)

We define restite minerals as those minerals, present in the protolith prior to partial melting, that survive as the refractory residua of partial melting. Table 1 lists several melting reactions in which aluminosilicate (Als) is part of the original subsolidus mineral assemblage of the (metapelitic) protolith. Given the low *T*–low *P* stability region of andalusite, and its limited region of overlap with the field of granite magmas, andalusite is an unlikely phase to occur as part of a truly restitic assemblage in many granitoid magmas, especially if extensive partial melting has taken place at high temperatures. Fluid-present melting reactions with $(H_2O)_v$ are likely to be lower *T*, and Als = andalusite. Fluid-absent melting reactions, especially those involving biotite dehydration, are likely to be high *T*, and Als = sillimanite. Depending on the bulk

composition of the protolith, and the degree of partial melting, Als can remain as part of the restitic refractory residuum. If any magma had been in equilibrium with andalusite as a restite phase in the region of partial melting, that magma would be saturated in andalusite, and would probably remain saturated during its ascent to lower pressures. Such magmas are strong candidates for crystallizing magmatic andalusite (below).

Distinguishing between former restitic andalusite and new magmatic andalusite is extremely difficult, especially in the absence of melt inclusions. Andalusite-bearing surmicaceous enclaves may be restites from the source area (Didier, 1991; Montel *et al*., 1991; Gaspar & Inverno, 1998), but in the absence of minerals or textures typical of high temperatures and pressures (Wall *et al*., 1987), such enclaves are more likely to be partially digested xenoliths of country rocks. Unless some of our andalusites represent disaggregated relicts from such enclaves, restitic andalusite must be rare.

Table 1: Examples of melting reactions involving aluminosilicate (Als) as an original phase of the protolith

Bt + Als + Qtz + Kfs + H_2O_v → L
Als + Bt + H_2O_v + Kfs + Pl + Qtz → L
Als + Bt + H_2O_v + Kfs + Ms + Qtz → L
Bt + Als + Qtz + Pl + H_2O_v → L + Grt/Crd
Bt + Pl + Ksp + Qtz + Als + H_2O_v → L
Bt + Als + Qtz + H_2O_v → L + Crd
Bt + Als + Qtz + H_2O_v → L + Grt
Grt + Als + Kfs + Pl + Qtz + H_2O_v → L + Bt
Als + Kfs + Qtz + H_2O_v → L
Bt + Qtz + Als → L + Grt + Kfs
Bt + Pl + Qtz + Als → L + Grt/Crd + Kfs
Als + Qtz + Kfs + Pl → L

L, silicate melt.

Type 2 Magmatic (melt phase an integral part of the formation of andalusite)

Type 2a Magmatic–peritectic (T↑)

Table 2 lists several reactions in which andalusite appears solely as the result of melt-producing reactions in originally andalusite-free rocks. In none of these reactions is andalusite also present in the subsolidus mineral assemblage, but it appears peritectically in an incongruent melting reaction. We regard such andalusite as being magmatic because, in phase equilibrium terms, it demonstrates a stability field overlap with a silicate melt.

High-temperature fluid-absent melting reactions will favour Als = sillimanite, but low-temperature, low-pressure, water-saturated melting reactions will favour Als = andalusite. Spatially, andalusite of this type may form along the contact between pelitic xenoliths and melt, or associate with the melt phase (initially as leucosomes) rather than the refractory residuum (restite) in anatectic migmatites. Such andalusites have no subsolidus metamorphic history, and thus may be euhedral and free of the mineral inclusions metamorphic andalusites commonly contain. Kawakami (2002) has described andalusite of magmatic origin from migmatites in Japan. Small crystals of euhedral andalusite in some Himalayan leucogranites are surrounded by thin rims of sillimanite (Castelli & Lombardo, 1988; Visonà & Lombardo, 2002), and may be the products of a *T*↑ (rising temperature) peritectic melt-producing reaction. In such a reaction, andalusite initially grows in the metapelites by peritectic melting reactions and replacement by topotactic sillimanite is the result of rising temperature (e.g. Cesare *et al.*, 2002).

Table 2: Examples of reactions that produce aluminosilicate (Als) only as a result of peritectic melting relations

Ms + Bt + Pl + Qtz + H_2O_v → L + Als
Grt + Crd + Kfs + H_2O_v → L + Als + Bt
Crd + Pl + Kfs + Qtz + H_2O_v → L + Als
Ms + Qtz ± H_2O_v → L + Als + Kfs
Bt + Crd → L + Als + Grt + Qtz
Qtz + Ksp + Bt → Als + L
Ms + Pl + Qtz → L + Kfs + Als
Ms + Qtz → L + Als + Kfs + Bt

L, silicate melt.

Prime candidates for *T*↑ peritectic andalusite occur in the migmatites from our sample set. Sample RIC-06 shows abundant large andalusite crystals growing along the leucosome–melanosome contact, and samples CLR-01 (Fig. 4a) and CLR-02 also have high modal abundances of andalusite in the

leucosomes. Such high concentrations of andalusite in early melts are important in considering the origin of andalusite in all felsic igneous rocks. Furthermore, the coarse grain size of some of these andalusites is normal for leucosomes (Kriegsman, 2001). Cesare *et al*. (2003) regarded andalusites with melt inclusions as having formed in xenoliths during peritectic melting reactions, and subsequently having been released into the main magma by disaggregation of the xenolith. Sample BAR-01 (Fig. 3e) may also have formed in this way, and is now in a melt with which it is not in equilibrium, hence its irregular grain shape and reaction rim of cordierite. This reaction is the up-temperature reverse of the andalusite-forming reaction (Type 2b) below.

Type 2b Magmatic–peritectic, (T↓), water-undersaturated
A second, much more restricted, type of peritectic magmatic reaction occurs in which andalusite appears as a result of *T*↓ (falling temperature) in a water-undersaturated melt-solid reaction such as

$$\mathrm{L} + \mathrm{Crd} \rightarrow \mathrm{And} + \mathrm{Bt} + \mathrm{Plag} + \mathrm{Qtz}\ [+\ (\mathrm{H_2O})_\mathrm{v}]\,.$$

The andalusite so produced may be chemically, although perhaps not texturally, indistinguishable from Type 2c andalusites below. In the Cooma 'granodiorite' (Chappell *et al*., 1991), which is more like a heterogeneous diatexite than a granodiorite, andalusite occurs in biotite reaction rims around cordierite macrocrysts. Ellis & Obata (1992) described the origin of that andalusite as a typical back-reaction when the melting reaction was reversed. Samples CLA-07 (Fig. 13a) to CLA-10, inclusive, from the Musquodoboit Batholith (Abbott & Clarke, 1979), also represent this down-temperature peritectic reaction.

Type 2c Magmatic–cotectic (T↓ and/or P↓), water-undersaturated
Any overlap between the stability fields of andalusite and granitic magmas means that andalusite can become saturated in a silicate melt of appropriate composition. Aluminosilicate saturation in the melt phase is favoured by excess alumina (high A/CNK), and must be achieved by some closed- or open-system process, or combination of processes, such as source inheritance, fractional crystallization, contamination, or possibly water saturation and escape of a fluid phase. Figure 1b shows that isobaric cooling might produce andalusite in upper-crustal magmas (coarse-grained granitoids), and that adiabatic pressure decreases are capable of producing andalusite in rapidly ascending magmas (aplites and volcanics).

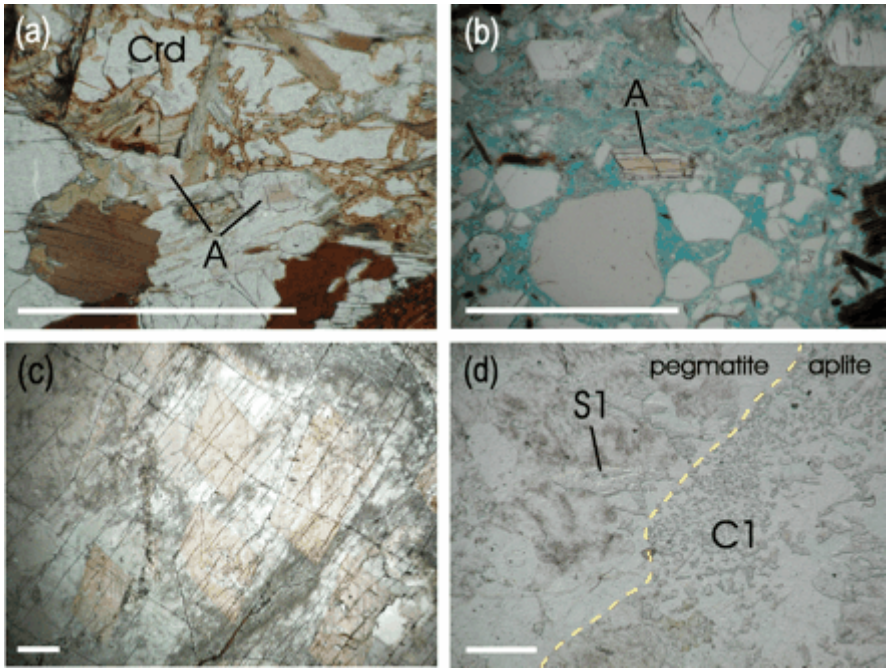


Fig. 13. Photomicrographs illustrating andalusite textures with genetic significance. (a) Sample CLA-07 (granite; Musquodoboit Batholith, Nova Scotia) shows reaction rims of andalusite and biotite on cordierite. (b) Sample MOR-01 (rhyolite; Morococala, Bolivia) shows a single fragmented andalusite in a crystal tuff. (c) Sample GOM-13 (aplite–pegmatite; Penafiel, Portugal) shows an apparent cluster of pink andalusite cores overgrown by colourless andalusite. (d) Sample JAM-03 (aplite–pegmatite; South Mountain Batholith, Nova Scotia, Canada) shows a contact between textural type S1 andalusite-bearing pegmatite (upper left) and textural type C1 andalusite-bearing aplite (lower right). Scale bars represent 1 mm.

With a significant field of overlap between the stability fields of andalusite and granitic melts in *T–P* space, and with andalusite stable down to the solidus temperature in most cases, the general andalusite-forming reaction must be

$$\mathrm{L} \rightarrow \mathrm{And} + \mathrm{Kfs} + \mathrm{Plag} + \mathrm{Qtz} + \mathrm{Other\ Magmatic\ Solid\ Phases.}$$

The problem is to distinguish this primary magmatic cotectic andalusite from all other possible origins.

The euhedral, or mechanically fragmented, andalusite crystals in volcanic rocks [Macusani sample LON-01 (Fig. 3a), Macusani sample PIC-01 (Fig. 8), and Morococala sample MOR-01 (Fig. 13b)] are strong candidates for a primary cotectic magmatic origin. According to Pichavant *et al.* (1988), the Macusani magma crystallized at T ~650°C, P = 1·5–2·0 kbar, and a_{H2O}~1 and the andalusite at 1·5–1·75 kbar. For the andalusite-bearing rhyolites of Morococala, Morgan *et al.* (1998) estimated andalusite formation at 740–750°C and a pressure ≤4–5 kbar. Some Morococala rocks contain muscovite rather than andalusite, suggesting a pre-eruption increase in a_{H2O} to drive the And + Kfs + $(H_2O)_v$ reaction to Qtz + Ms.

Type 2d Magmatic–cotectic ($T\downarrow$ and/or $P\downarrow$), water-saturated
Almost every felsic magma reaches water saturation at some temperature above the solidus. These low-temperature, water-saturated, conditions favour maximum overlap with the andalusite stability field. Water saturation could occur with, or without, andalusite already present in the system, and the occurrences of andalusite in pegmatites, and even quartz veins (Whitney & Dilek, 2000) demonstrate its ability to nucleate and grow in a water-saturated environment. Andalusite can occur in small pegmatitic melt pods in andalusite-bearing granulite-facies rocks (Vernon & Collins, 1988), or in large zoned pegmatites associated with peraluminous granitoids (Voloshin & Davidenko, 1973; Leal Gomes, 1984). Individual andalusite crystals may range in size from micrometres to metres, and they commonly occur near the quartz-rich and alkali-deficient (least likely magmatic) cores of the pegmatites in association with other characteristic peraluminous minerals (e.g. spinel, corundum, dumortierite, topaz, pyrophyllite, and diaspore).

General crystallization sequences for andalusite formation are

$$\begin{aligned} &\mathrm{L} \pm \mathrm{Solids} \rightarrow \mathrm{L} \pm \mathrm{Solids} + \mathrm{Andalusite} \\ &\rightarrow \mathrm{L} \pm \mathrm{Solids} + \mathrm{Andalusite} + \mathrm{Aqueous\ Fluid} \end{aligned}$$

$$\begin{aligned} &\mathrm{L} \pm \mathrm{Solids} \rightarrow \mathrm{L} \pm \mathrm{Solids} + \mathrm{Aqueous\ Fluid} \\ &\rightarrow \mathrm{L} \pm \mathrm{Solids} + \mathrm{Aqueous\ Fluid} + \mathrm{Andalusite} \end{aligned}$$

$$\begin{aligned} &\mathrm{L} \pm \mathrm{Solids} \rightarrow \mathrm{L} \pm \mathrm{Solids} \\ &+ \mathrm{Aqueous\ Fluid} + \mathrm{Andalusite}. \end{aligned}$$

The first case is just a continuation of Type 2c above, namely the magma became fluid-saturated after andalusite crystallization had begun. Mantling of these andalusites with magmatic muscovite may follow. In the second case, the creation of a separate aqueous fluid phase precedes the formation of andalusite, and that fluid phase may, or may not, be instrumental in the formation of andalusite in that particular system. The aqueous fluid phase is also significant in that it facilitates chemical migration of elements to produce the large andalusite crystals characteristic of some pegmatites. Large crystals of andalusite in coarse-grained pegmatites include sample GOM-13 with euhedral pink cores (Fig. 13c), and sample TOS-05 (Fig. 4b) with an apparent reaction relationship between early andalusite and later, but still primary, muscovite. Andalusite in sample CLA-12 (Fig. 3c) occurs as apparent clusters

of optically continuous grains that are probably large single skeletal crystals (Clarke *et al.*, 1998).

Sample JAM-03 (Fig. 13d) shows andalusite occurring on both sides of an aplite–pegmatite contact: single large textural type S1 crystals on the pegmatitic side, and clusters of small textural type C1 crystals on the aplitic side. The environment of crystallization seems to be similar to that produced by periodic build-up and release of fluids described by Lowenstern & Sinclair (1996). The large S1 single andalusite crystals in the pegmatite appear to have grown from the water-saturated melt under static conditions. The small C1 clusters in the aplite may have grown as the result of periodic buildup and release of water pressure resulting in saturation of Al_2SiO_5 in the silicate melt, either by removal of alkalis from the melt (Clarke, 1981), or by decreasing the water and alumina solubility in the melt (Acosta-Vigil *et al.*, 2003). Thus, the andalusite in the aplite may be the result of combined pressure quenching and compositional oversaturation. Significantly, sample JAM-03 may be a macrocosm for what happens in the final interstitial melt of crystallizing granites to produce fine-grained C1, C2, and C3 clusters of andalusite.

Type 3 Metasomatic (melt phase absent, fluid phase present)
Type 3: Metasomatic
Metasomatic andalusite in felsic igneous rocks is rare, requiring the removal of Ca–Na–K from the solid rock by aqueous fluids. Such andalusite should be associated with a subsolidus hydrothermal alteration process. Few examples of metasomatic andalusite exist in the literature; however, Corey (1988) described a high-alumina hydrothermal alteration zone in the South Mountain Batholith containing And + Sil + Spl + Ms + Crd + Ap + Pyr. Sample CLA-05 (Fig. 9a) comes from the same locality. What is remarkable about this sample is its high modal abundance of andalusite, otherwise the grain sizes, grain shapes, and oscillatory chemical zoning satisfy the conditions to be primary magmatic. This sample is also unusual because its coexisting biotite–muscovite tie line (Fig. 11b) lies at the lowest F content of our entire spectrum of samples. In this regard, it is similar to the Cooma and Mt. Stafford migmatites representing early, low-F, andalusite-rich partial melts, and we propose that sample CLA-05 is an extensively melted metapelite.

Several types of andalusite can cross physical and, therefore, classificatory boundaries. For example, a Type 2a magmatic peritectic andalusite, formed in an incongruent melting reaction, may become a Type 1c xenocrystic andalusite in another magma (e.g. BAR-01); a Type 2a magmatic peritectic andalusite, formed during a melting reaction, may become a Type 2c magmatic cotectic andalusite after more extensive melting; or a Type 1c metamorphic xenocrystic or Type 1d metamorphic restitic andalusite may also become the core of a later overgrowth of Type 2c magmatic cotectic andalusite. Restitic (and xenocrystic) andalusite could become magmatic Type 2c instead of metamorphic as it equilibrates with a granitic melt (but not by direct crystallization from it). In short, a single andalusite grain may have

had a lengthy history, and some or all of the evidence of its former incarnations is overwritten.

Classification and origin of andalusite in the sample set

Electronic Appendix Table A6 shows the key textural and chemical characteristics of the 108 andalusite-bearing felsic igneous rocks in our sample set and the most probable origin of the andalusite in each sample.

The magmatic case

In general, the evidence in favour of magmatic andalusite includes:

1. presence of melt inclusions in andalusite;
2. euhedral grain shapes of andalusite, especially in volcanic rocks and aplites;
3. grain-size compatibility with minerals acknowledged to be magmatic;
4. coexisting biotite with $Al^{iv} \approx 2{\cdot}68 \pm 0{\cdot}07$;
5. coexisting biotite–muscovite–apatite in chemical (and probably magmatic) equilibrium;
6. zoning in andalusite that resembles zoning in other magmatic phases.

Table 3: Numbers of samples with magmatic textural and/or chemical characteristics

Characteristic	Number	Comment
Grain size		
Andalusite compatible with accepted magmatic minerals	52	
Andalusite smaller than accepted magmatic minerals	45	
Grain shape		
Euhedral–subhedral	23	
Aggregation		
Textural type S only	43	all volcanic rocks, and 8 of 12 migmatites
Textural type C only	29	of which 23 are plutonic rocks
Textural types S and C in same rock	27	of which 16 are plutonic rocks
Inclusions		
Melt inclusions or polycrystalline inclusions	13	
Zoning		
Sharp concentric, sector, or oscillatory zoning	27	
Mineral compositions		
Samples with biotite with $Al^{iv} \sim 2{\cdot}68$	68	
Coexisting equilibria		
Biotite–muscovite in Ti equilibrium	27	
Biotite–muscovite in F equilibrium	46	

On the strength of this evidence, we conclude that 99 andalusite-bearing samples in Electronic Appendix Table A6 and in Table 3 have one or more textural or chemical criteria to suggest that they are Type 2a–2d magmatic in origin, i.e. the andalusite grew from, or at least in the presence of, a silicate melt phase. We recognize a fundamental petrogenetic difference between the size-compatible single andalusite grains (textural type S; Fig. 6) and the size-incompatible (small) clustered andalusite grains (textural type C; Fig. 6). Textural type S single grains of andalusite may represent Al_2SiO_5 saturation in the melt before water saturation, resulting in normal primary magmatic crystallization, whereas textural type C clusters of andalusite grains may represent water saturation before Al_2SiO_5 saturation, resulting in fine-grained 'quench' clusters of andalusite.

The xenocrystic case

The textural parameters of andalusites that we have used (size, shape, inclusions, state of aggregation, relation to muscovite) are open to alternative explanations. Grains with anomalous sizes, shapes, inclusions, and/or textural relations with magmatic rock-forming minerals (or other metamorphic minerals) are likely to be Type 1c xenocrystic (e.g. BBR-01,02 based on anomalously large size, irregular shape, chiastolite inclusions, and obvious reaction rims). General arguments in favour of a xenocrystic origin for andalusite include:

1. euhedralism is not an exclusively magmatic texture;
2. many peraluminous granite magmas originate at depths incompatible with andalusite stability;
3. the range of *T–P–X* conditions for xenocrystic andalusite in granites is greater than the range of *T–P–X* conditions for magmatic andalusite in granites;
4. the whole-rock A/CNK parameter is irrelevant if the andalusite in the rock is xenocrystic, and it carries little or no weight when the origin of the andalusite is in doubt.

To illustrate the complexity of the problem of determining the origin of andalusite, we selected three specific examples (BAR-01, GOT-02, UGI-02 to 07) for a more detailed examination (Electronic Appendix Table A7). In each case, foreign material is clearly present in the rock, and the textural–chemical evidence for magmatic andalusite is equivocal; therefore, a xenocrystic origin for the andalusite is possible. The result of this type of detailed reconsideration of the observations for the entire sample set would be that the frequency of Type 1c may increase at the expense of Types 2a, 2c, and 2d.

Most of our samples appear to contain magmatic andalusite (Type 2a–d). The greatest problem is to distinguish between Type 2c cotectic magmatic, Type 2a peritectic, and Type 1c xenocrystic (if the assimilation of the foreign

andalusite is in an advanced stage). Logically, however, if andalusite in volcanics, aplites, pegmatites, and migmatites is magmatic, why should andalusite in compositionally equivalent medium- to coarse-grained granites be xenocrystic? Also, why should xenocrysts be of uniform size, and why should they cluster? And what special conditions must obtain to permit a euhedral andalusite xenocryst from the country rock to remain euhedral in a magma? Furthermore, Type 2a peritectic andalusite can only be positively identified in its migmatitic spatial context; some Type 2a andalusites, removed from their migmatitic origins, may be misclassified as Type 2c. Although these Type 2a peritectic melt reactions may produce abundant andalusite (e.g. CLR-01 and CLR-02), if these reactions were the principal method of generating andalusite, we might expect to find andalusite more commonly in peraluminous batholiths, unless it remained in the refractory residuum of partial melting or was incorporated into the melt at higher temperatures. Also, the high temperatures required to generate large quantities of granitic magma are inconsistent with andalusite being more abundant than sillimanite in felsic igneous rocks. Many felsic magmas must have been Al_2SiO_5-undersaturated while in the sillimanite stability field, and reached critical saturation in Al_2SiO_5 only at low temperatures in the andalusite stability field.

CONTROLS ON THE FORMATION OF MAGMATIC ANDALUSITE

Introduction

Most of the andalusites in our sample set satisfy one or more of the textural and chemical criteria for a magmatic origin. On this basis, the stability fields of andalusite and naturally occurring felsic magmas must overlap; however, many peraluminous felsic igneous rocks do not contain andalusite, and many plutons do not contain andalusite throughout, but rather only in restricted facies. Special conditions must obtain for the formation of that andalusite (Clemens & Wall, 1981, 1988; Patiño Douce, 1992). In this section, we focus on the variables that may contribute to the formation of magmatic andalusite in felsic igneous rocks.

Conditions favourable for the formation of magmatic andalusite

Attaining the critical A/CNK ratio in the melt composition

Metaluminous felsic igneous rocks do not contain primary magmatic andalusite, but peraluminous felsic igneous rocks can. (If the andalusite is magmatic, its crystallization should be the consequence of high A/CNK in the bulk magma composition; however, if the andalusite is xenocrystic, the high A/CNK in the bulk rock may be merely an artifact caused by the addition of andalusite and other peraluminous phases.) The effect of excess alumina in a magma is two-fold: (1) it creates a more favourable *T*–*P* range for andalusite

crystallization by depressing the granite solidus (Abbott & Clarke, 1979; Holtz *et al*., 1992; Joyce & Voigt, 1994), enlarging the region of overlap with the andalusite stability field; (2) it creates a more favourable compositional condition because, the more peraluminous a magma is, the greater is the probability that it will become saturated in Al_2SiO_5 and crystallize andalusite. Halliday *et al*. (1981) described a number of processes by which a magma can increase its peraluminosity. In this section, we focus on three compositional conditions to enhance the crystallization of andalusite.

Inheritance of A/CNK from the source region. A magma with a high initial A/CNK [$(A/CNK)_i$] inherited from pelitic source rocks will favour crystallization of andalusite. Assimilation of highly peraluminous country rocks may also produce the same effect on alumina saturation, but may result in xenocrystic andalusite rather than magmatic andalusite. In such cases, the source or contaminant controls the peraluminous character of the melt. Progressively more peraluminous melts will be produced in equilibrium with the following residual assemblages: (a) biotite; (b) biotite + garnet; (c) biotite + cordierite; (d) biotite + andalusite/sillimanite/kyanite. In the last case, the melt is already saturated in Al_2SiO_5 at the time of segregation from the source rocks, and as long as that saturation is maintained, the appearance of andalusite on the liquidus is inevitable (provided the *T*–*P* path of the magma passes through the andalusite stability field). Andalusites produced in magmas such as these would be Type 2a peritectic and Type 2c cotectic (e.g. the Macusani volcanics).

Increase of $(A/CNK)_i$ by feldspar fractionation. Large volumes of partial melt derived from mixed metapelite–metagreywacke sources will have A/CNK >1, but may also be undersaturated in Al_2SiO_5. At what value of A/CNK does a magma reach saturation in Al_2SiO_5? From experimental studies, melts approaching equilibrium with Al_2SiO_5, or other strongly peraluminous phases, have A/CNK values of *c*. 1·30–1·35 (Joyce & Voigt, 1994; Scaillet *et al*., 1995). Similarly high A/CNK values also occur in melt inclusions in quartz in the Morococala volcanics. For those of our samples for which we have whole-rock chemical analyses, the mean A/CNK value is 1·19 ± 0·08, indicating that many samples have values lower than those suggested by experimental work as being necessary to saturate a magma in aluminosilicate.

The question is: can a low A/CNK melt evolve to A/CNK levels high enough to nucleate Type 2c cotectic andalusite? For any melt with A/CNK >1 that is fractionating feldspars only, the mole fraction of alumina in the melt that is not charge balanced by alkalis doubles for every 50% of fractional crystallization.

Table 4: Amount of fractional crystallization of feldspars required to reach A/CNK = 1·20 and 1·30 from magmas with a range of $(A/CNK)_i$ compositions

$(A/CNK)_i$	% $Cryst_{1.20}$	% $Cryst_{1.30}$
1·02	90	93
1·05	75	83
1·10	50	67
1·15	25	50
1·20	0	33

Table 4 shows the percent of such feldspar crystallization required to reach two levels of A/CNK (1·20 and 1·30). If the $(A/CNK)_i$ in the magma is sufficiently high (last row), little or no fractional crystallization is needed to reach Al_2SiO_5 saturation. Monomineralic andalusite zones in the D5 pegmatite at Arreigada, Pacos de Ferreira, Portugal (Electronic Appendix Table A1) appear to have formed as the result of feldspar fractionation (Leal Gomes, 1984). The mean A/CNK values in the South Mountain Batholith, Nova Scotia, range from 1·16 in early granodiorites to 1·23 in late leucogranites (Clarke *et al*., 2004), and many of its moderately evolved rocks contain andalusite (samples CLA-01 to 14, ERD-01, JAM-03). The discrepancy between the A/CNK required to nucleate andalusite in natural and synthetic systems can be reconciled if the naturally occurring andalusite grows as a late product from a more highly evolved interstitial melt.

Values are calculated using the Rayleigh fractionation equation $C_L = C_o(F^{D-1})$, where C_L is the final excess alumina in the melt, C_o is the initial excess alumina in the melt, F is the melt fraction remaining, and $D = 0$.

Although, theoretically, feldspar fractionation can drive all $(A/CNK)_i$ >1 melts to Al_2SiO_5 saturation, in practice saturation with, and fractionation of, other phases such as cordierite, biotite, and muscovite will retard, or even prevent, the magma from reaching saturation in andalusite. Conversely, contamination with pelitic material may assist the increase in A/CNK. If fractional crystallization is responsible, andalusite will be restricted to those parts of the intrusion that are chemically highly evolved, or to the last interstitial melt. This prediction is in general agreement with other indices of fractional crystallization such as low concentrations of compatible elements (Ti, Sr, Zr, Ba) and high concentrations of incompatible elements (Rb, Cs, Li) in andalusite-bearing facies of peraluminous plutons.

Increase of $(A/CNK)_i$ by evolution of an aqueous fluid phase. The common occurrence of andalusite in aplites (Figs 3b, c, 5b and 13d), which are normally associated with fluid-saturated pegmatites, and in fluid-saturated pegmatites themselves (Figs 4b, 9d, and 13c and d), suggests a role for fluids in the production of andalusite. The large euhedral crystals of andalusite in

some pegmatites (TOS-05, Fig. 4b; GOM13, Fig. 13c; JAM-03, Fig. 13d) show that andalusite is stable with hydrothermal fluids (Cesare, 1994; Whitney & Dilek, 2000), and that andalusite does not react under all conditions to become secondary muscovite. Any andalusite formed under such conditions would be Type 2d water-saturated magmatic.

We now consider whether some fluid-related process could be effective in attaining the A/CNK levels necessary to crystallize andalusite.

(1) *Effect of water on shifting primary phase volumes*. In general terms, the appearance of a stability field for a fluid phase will have an effect on the sizes, shapes, and positions of the primary phase volumes for all other phases, including andalusite. The effect of such reconfiguration of the liquidus topologies on the probability of crystallizing andalusite in complex natural systems is unknown.

(2) *Effect of water on stripping alkali elements from the melt*. Evolution of a separate water-rich fluid phase ($a_{H2O} \leq 1$) has the potential to raise the A/CNK of the silicate melt from which it evolves by preferential partitioning of Na and K into the fugitive fluid phase. This process could potentially take the melt composition to 'hyperaluminous' A/CNK levels unattainable by melt–solid equilibria (Clarke, 1981). Evidence of high degrees of alkali-element mobility in fluid phases in plutons includes saline fluid inclusions (Na, K, Cl removal), albitization (Na addition), and greisenization (K addition).

Is vapour saturation and consequent alkali partitioning, or stripping, an adequate mechanism for achieving aluminosilicate saturation in felsic melts? In a worst-case scenario, calculations for the haplogranite minimum composition $Ab_{39}Or_{26}Qz_{35}$ (wt %), A/CNK = 1, and 5·5 wt % H_2O (near saturation at 2 kbar), show that if all of the water in the haplogranite minimum melt were to exsolve as a single batch, it would require $D_{Na}^{vapour/melt} = D_{K}^{vapour/melt} \approx 3–4$ to reach A/CNK ≈1·30. These *D* values appear to be too high, given that work with macusanite indicates $D_{Na}^{vapour/melt}$ and $D_{K}^{vapour/melt}$ to be of the order of 0·1 (London *et al*., 1988), approximately an order of magnitude lower than the value estimated for the Spoor Mountain rhyolite (Webster, 1997). Even assuming *D* values of unity, complete vapour exsolution would change the A/CNK from 1·00 to *c*. 1·06, clearly insufficient if $(A/CNK)_i$ were so low, but much more effective if A/CNK of the melt were ≥1·20 when water saturation occurred.

An alternative is to consider the role of chlorine in complexing Na and K in the vapour phase. When $D^{vapour/melt} = 1$, a fluid with 14 wt % NaCl + KCl requires 0·475 g of Cl per 5·5 g of H_2O. This amount of Cl exceeds the known solubility of Cl in H_2O-saturated (in fluid approaching unity) melt by a factor of ~2, and also greatly exceeds the known solubility of Cl in anhydrous granitic melts. As shown by Webster (1997), the solubility of H_2O in haplogranitic melt at 2 kbar decreases from about 5·5 wt % at ~0·2 wt % Cl in the melt to essentially 0 wt %

H_2O at ~0·3 wt % Cl in melt. Rayleigh fractionation of Cl-complexed alkalis into a highly mobile fluid phase can, at least to some extent, enrich the residual silicate melt in A/CNK and, depending on the A/CNK of the melt at the time of water saturation, take the silicate melt over a critical threshold to Al_2O_5 saturation, or possibly even to A/CNK compositions unreachable by melt–solid equilibria alone.

Most felsic magmas that evolve a separate aqueous fluid phase never nucleate andalusite, so water saturation alone is not a sufficient condition to form primary magmatic aluminosilicates. If the fluid saturation occurs while the magma is inside the andalusite *T–P* stability field, andalusite may nucleate if the A/CNK of the melt reaches saturation in Al_2SiO_5.

(3) *Effect of water on Al solubility in silicate melts*. The experimental work of Acosta-Vigil *et al*. (2002, 2003), based on saturating haplogranite starting materials individually with a variety of aluminous phases, shows that alumina solubility in the melt depends on the coexisting phase, the temperature, and the water content of the melt. In particular, the positive correlation between X_{H2O} and A/CNK suggests that alumina solubility is a direct function of water content of the melt phase. Thus, alumina solubility in the melt is maximized at high water contents, and decreases when that water is released (and when the temperature falls). The loss of aqueous fluid from the melt, and reduction of water content of the melt, reduces the solubility of alumina and results in the crystallization of a phase with A/CNK >1. The particular peraluminous phase that crystallizes is determined by the precise phase relations for that *T–P–X* condition. Under suitable conditions, that phase could be andalusite, or some other peraluminous phase such as garnet or cordierite (Rapela *et al*., 2002).

In conclusion, if a spatial–temporal–genetic correlation of fluids and andalusite exists in plutons as a whole, then high A/CNK levels in the granitic rocks, and the appearance of primary magmatic andalusite, may lie close to the region of initiation of water saturation. This andalusite-in 'isopleth' in plutons represents the place where vapour saturation has driven the composition of the melt phase against the andalusite primary phase volume. The appearance of (water-saturated) magmatic andalusite in one place in a pluton, and the occurrence of sub-solidus alkali metasomatism in another place (albitization, K-feldspathization, and greisenization) could be complementary processes in the late stages of evolution of peraluminous granites. As a consequence, the same fluids that are indirectly responsible for the formation of andalusite in aplite–pegmatite systems in one part of a pluton might destroy Types 1a–2c andalusite elsewhere in the same pluton.

Lowering of the granite solidus

Even with a suitable A/CNK ratio, andalusite will not crystallize from a felsic melt unless the stability field of andalusite overlaps that of the melt. In this section, we consider several ways in which the granite solidus may be

lowered (beyond the effect of high A/CNK itself) to increase the probability of overlap with the stability field of andalusite.

High concentrations of Be–B–Li. In general, high concentrations of Be–B–Li in granitic rocks are normally associated with pegmatites, and those pegmatites can contain andalusite. An example is the Alburquerque pluton, Spain (London *et al*., 1999). In it, only the marginal granites contain andalusite, whereas the pegmatitic facies and dykes do not. Remarkably, the pegmatites have much higher A/CNK ratios than the associated granites. The high Be–B–Li content appears to stabilize other Al-rich phases (beryl, tourmaline, spodumene), instead of andalusite. In general, the effects of high concentrations of the light elements (Be, B, Li) are opposing: (1) increasing the probability of stabilizing primary magmatic andalusite by lowering the granite solidus (Fig. 1), but (2) decreasing the probability of stabilizing primary magmatic andalusite by diverting Al from potential andalusite into such minerals (or chemical components) as beryl, tourmaline, spodumene, and berlinite.

Although the effect of beryllium is to lower the haplogranite solidus slightly (Evensen *et al*., 1999) into the andalusite stability field, the effect of beryl crystallization would be to reduce A/CNK in the melt and diminish the probability of nucleating andalusite. None of our samples shows any obvious mineralogical evidence of high Be contents, thus we judge that this element is not a factor in promoting the presence or absence of andalusite in our sample set.

The effect of high levels of boron is to depress the haplogranite solidus by several tens of degrees Celsius (Chorlton & Martin, 1978; Manning & Pichavant, 1983; Acosta-Vigil *et al*., 2001; Kawakami, 2001), thereby expanding the region of overlap with the andalusite stability field. However, the precipitation of tourmaline might be expected to lower the A/CNK of the silicate melt, and diminish the probability of nucleating andalusite. If high levels of boron were responsible for the formation of andalusite in most of our samples, little mineralogical evidence of its presence exists in our sample set; nevertheless, seven of our andalusite-bearing rocks (GOM-04, JAM-03, RIC-03, RIC-04, UGI-03, VIL-03, and VIS-03) do contain texturally compatible tourmaline, suggesting that, in these rocks at least, the positive effect of boron on lowering the granite solidus was greater than the negative effect of Al-diversion to tourmaline.

As with the other light-element cations, the effect of lithium is to lower the haplogranite solidus by several tens of degrees Celsius (Wyllie & Tuttle, 1964; London & Burt, 1982; Martin & Henderson, 1984), thereby expanding the primary phase field of andalusite. Lithium is also able to sequester Al in, for example, spodumene or amblygonite otherwise possibly destined to become primary aluminosilicate minerals.

The only sample from a pluton with measured lithium contents in its micas is KOL-01 (Bt with 1100 ppm Li, and Ms with 500 ppm Li). Otherwise, the equations of Tischendorf *et al.* (1997, 1999) yield the following estimates for lithium (Li_2O wt %) contents in the micas of our sample set: biotite—range 0·12–1·15, mean 0·28 ± 0·19; muscovite—range 0·02–1·27, mean 0·18 ± 0·19. If the K_D^{Li} between muscovite and melt is ~0·5 (Walker *et al.*, 1989), the melt compositions contained roughly double the Li_2O concentrations estimated for the muscovite samples. Our sample set shows no obvious mineralogical evidence of high lithium contents, and the only effect of its presence is to have a small effect on lowering the granite solidus. High lithium contents, therefore, do not seem to be essential to the appearance of andalusite in felsic igneous rocks.

High concentrations of P. The presence of phosphorus has a complex effect on the effective value of A/CNK in the silicate melt phase. In general, the higher the P content of the whole rock, the higher the true A/CNK must have been in the melt because phosphorus decreases the Ca term in the denominator by an amount equivalent to 3·3 P. However, another effect is the amount of P in the feldspars (Kontak *et al.*, 1996). Through the berlinite substitution, $Al^{3+}\ P^{5+} \rightleftharpoons 2Si^{4+}$, A/CNK >1 in fractionating feldspars, and thus the effect of P is to reduce the effectiveness of feldspar fractionation to increase A/CNK in residual melts. Also, if P and Al form discrete anionic complexes that do not co-polymerize with the principal aluminosilicate framework of the melt, the net effect of increased P (at constant Al) is a decrease in a_{Al2O3}. In this case, it will require a higher A/CNK to produce saturation in an aluminous phase such as andalusite. The one environment in which this effect may be important is in highly fractionated pegmatite systems, where Al–P-rich derivative liquids also concentrate enough other lithophile components to stabilize late-stage phosphates [e.g. childrenite ($FeAlPO_4(OH)_2.H_2O$, lithiophilite ($LiMnPO_4$)–triphylite ($LiFePO_4$), and triplite $(Mn,Fe^{3+},Mg,Ca)_2(PO_4)(F,OH)$], which may then liberate complexed Al and increase a_{Al2O3}. This process could, at least in part, lead to late-stage precipitation of aluminosilicates.

High concentrations of F. The effect of F is to lower the granite solidus (Manning & Pichavant, 1983), thereby expanding the andalusite primary phase volume. Clemens & Wall (1988) suggested that high fluorine contents should stabilize And + Bt relative to Grt/Crd + Kfs. Our extensive chemical data permit several observations and deductions about the role of fluorine in the formation of andalusite in felsic igneous rocks, as follows.

(1) The extremely wide range of fluorine contents in our andalusite-bearing granitoids suggests that F concentration, at least alone, is not the controlling factor in the appearance of andalusite.

(2) Figure 11b illustrates the pseudo-binary muscovite–biotite system showing that the concentration of fluorine correlates with the degree of mutual solubility of the two micas. In the multicomponent natural system, the

presence of fluorine must modify the sizes, shapes, and positions of the primary phase volumes of biotite and muscovite. If they change, then so must also the primary phase volumes of coexisting phases such as andalusite, cordierite, garnet, etc. The implication of such changes in the topology of the relevant natural phase diagram is to change the probability, and order, of crystallization of all phases, including andalusite. High F contents will stabilize muscovite to higher temperatures, thereby shrinking the andalusite primary phase volume.

(3) The high F contents of the biotites in two of the volcanic samples (MOR-01 and PIC-01, Electronic Appendix Table A2) may indicate, however, that fluorine has a role in expanding the andalusite primary phase field at low-pressure, water-undersaturated conditions.

(4) At higher concentrations of fluorine, topaz appears to form instead of andalusite (London *et al.*, 1999, 2001; Neves *et al.*, 1999; Clarke & Bogutyn, 2003). Some peraluminous felsic igneous rocks should show evidence of the peritectic reaction

$$\mathrm{And} + \mathrm{F-rich\ Melt} \rightarrow \mathrm{Topaz}$$

but none is present in our sample set.

(5) At even higher fluorine contents, F may complex with Al and Na to form cryolite-like species that would decrease a_{Al2O3} in the silicate melt and decrease the probability of andalusite precipitation.

To summarize, our samples are probably representative of high A/CNK, andalusite-bearing rocks, but not necessarily all high A/CNK rocks. In most of our rocks, Be–B–Li–P appear not to be important chemical components, and we conclude that these elements may have had only a small effect on lowering the granite solidus to promote the formation of andalusite. Had we specifically investigated high A/CNK, high Be–B–Li–P, granites instead, we might have concluded that andalusite is only a rare mineralogical constituent, and that the negative effect of Be–B–Li–P on the formation of andalusite had prevailed because high concentrations of these elements lowered a_{Al2O3} and prevented formation of andalusite. In contrast, our samples contain a wide range of F contents (as deduced from the F concentrations in the micas). We conclude that fluorine is not necessary to stabilize andalusite, at least in plutonic rocks, and that high levels of fluorine serve to destabilize andalusite and form topaz, or to form complexes that reduce the probability of nucleating andalusite.

Expanding the andalusite stability field

Small amounts of transition-element solid solution in andalusite have a potentially significant effect on its *P–T* stability field (Grambling & Williams,

1985; Kerrick & Speer, 1988; Kerrick, 1990; Pattison, 1992, 2001; Fernández-Catuxo *et al.*, 1995), in particular by shifting the And = Sil boundary upward by 50–100°C. Although minor elements in andalusite may be important in stabilizing andalusite over sillimanite in some magmatic situations, many andalusites contain negligible concentrations of transition elements.

The andalusites with Fe-rich pink cores in our sample set (Figs 3–5, 8 and 9), including the completely pink andalusites in the Morococala volcanics, suggest that minor elements, such as Fe^{3+}, may be important in initially stabilizing andalusite or reducing its energy barrier for nucleation. Subsequent overgrowths of Fe-poor andalusite may take place more readily on the nuclei of Fe-rich andalusite, but the sharp core–rim compositional boundaries remain a problem. The general absence of a compositional gradient suggests that some *T–P–X* parameter changes abruptly.

Kinetic considerations

Pattison (1992) noted that, in metamorphic rocks, andalusite is a common metastable relict phase, persisting well upgrade of the first occurrence of sillimanite. If the And = Sil reaction is sluggish on geological time scales (10^5–10^7 years), it raises questions about the accuracy of laboratory determinations (e.g. ±25°C) on experimental time scales (10^{-2}–10^0 years), especially considering the difficulties of such work (Kerrick, 1990; Holdaway & Mukhopadhyay, 1993; Pattison, 2001). Samples NEV-04 and WHI-01 (Fig. 9f) show remarkable persistence of andalusite in the stability field of sillimanite.

In the case of rising temperature, magmatic andalusite may continue to grow in the stability field of sillimanite but, unless seeded, andalusite is unlikely to nucleate metastably in the sillimanite stability field. Interestingly, in the case of no overlap between the stability fields of granite melt and andalusite (Fig. 1a), moderate (20–50°C) to strong amounts of undercooling may result in stable, but rapid, growth of andalusite from metastable melt. Some of the andalusites in our samples do appear to have quench textures (CLA-12, ELB-01, ERD-01, JAM-03). They may be the result of rapid stable growth or rapid metastable growth, but they are almost certainly not xenocrystic.

PETROGENETIC MODEL

Of the many possible controls on the formation of andalusite in felsic magmas, the level of A/CNK and the effects of H_2O are probably the most important. Figure 14 summarizes the formation of magmatic andalusite under the most favourable conditions with a large *T–P* stability field for andalusite ('AND MAX') from Fig. 1b, utilizing the And = Sil curve of Richardson *et al.* (1969) and the most favourable melt composition (saturated in Al_2SiO_5 throughout). Whether

the And = Sil stability curve intersects the muscovite breakdown curve above the granite solidus (as the R69 curve does in Fig. 14), or below the granite solidus (as the P92 curve would do in Fig. 1a), is important to the petrogenetic interpretations that follow.

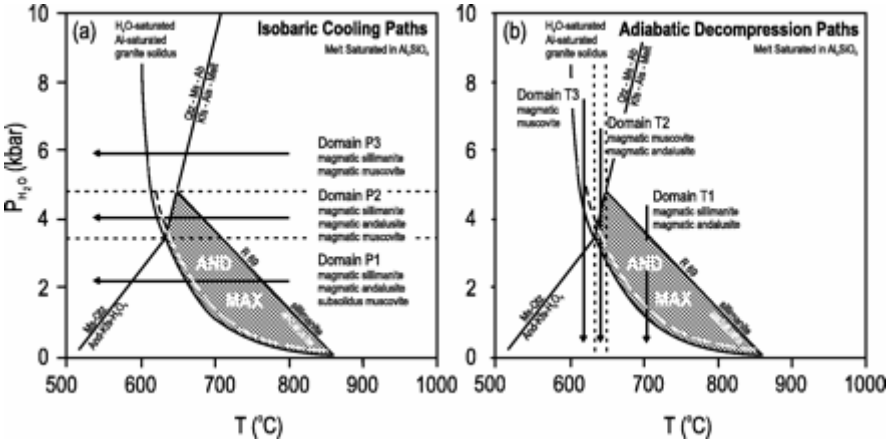


Fig. 14. Formation of magmatic andalusite in pressure–temperature space. In this petrogenetic grid for the formation of andalusite in felsic igneous rocks, the AND MAX field is defined by the water-saturated peraluminous granite solidus (Johannes & Holtz, 1996), the And = Sil reaction (R69; Richardson *et al.* 1969), and the stoichiometric muscovite breakdown curve. (a) Isobaric cooling paths. (b) Adiabatic decompression paths. Heavy dashed line is a schematic water-saturation curve for granitic melts.

The R69 case permits some, or all, of the muscovite rims on andalusite (Figs 4, 5 and 7) to be magmatic in origin; the P92 case restricts all the muscovite rims to be subsolidus in origin. Further work on the textures and compositions of those muscovite rims is needed to determine their origins, but the variation in their grain sizes and relations with the andalusite suggest that a single subsolidus origin is unlikely. Therefore, at least in some compositional situations, the And = Sil curve lies between P92 and R69 and intersects the muscovite stability curve above the granite solidus. Using the AND MAX field in Fig. 14 allows us to examine the implications of this situation.

Figure 14 subdivides the possible crystallization paths into two limiting categories: isobaric slow crystallization, and adiabatic rapid crystallization. Intermediate *T–P* paths combine features of these extremes. The isobaric crystallization paths (Fig. 14a) fall into three pressure domains, delineated by two critical invariant points. Isobaric cooling in the low-pressure Domain P1 results in magmatic sillimanite (if *T* were sufficiently high), followed by magmatic andalusite at temperatures closer to the solidus. Any muscovite in these rocks must be subsolidus. Isobaric cooling in the moderate-pressure Domain P2 results in magmatic sillimanite (again, if the temperature were sufficiently high), followed by magmatic andalusite. That andalusite then becomes involved in a peritectic reaction with the melt to produce magmatic muscovite. At this stage of our investigation, we do not know if a muscovite rim on an anhedral andalusite represents a slow peritectic partial resorption of a euhedral andalusite, or a fast overgrowth on an anhedral andalusite. Under conditions of perfect equilibrium crystallization, andalusite is

eliminated in this reaction, and all that remains is magmatic muscovite (Fig. 7a). Under conditions of perfect fractional crystallization, magmatic muscovite may overgrow, but not entirely replace, the andalusite. In the high-pressure Domain P3, andalusite never crystallizes, thus the invariant point at about 650°C and 4·8 kbar represents an upper pressure limit for the formation of magmatic andalusite.

The adiabatic decompression paths similarly consist of three domains (Fig. 14b). In the high-temperature Domain T1, the rocks may, or may not, show magmatic sillimanite followed by magmatic andalusite (possibly sample GOT-02) and the texture should be saccharoidal–aplitic or volcanic. Any muscovite in these rocks must be either subsolidus (not shown on the path), or grains crystallized at a higher pressure from a greatly expanded stability field (high Fe or F?). The greater the expansion of the muscovite stability field, the more andalusite crystallization is restricted to low pressures. In the extremely narrow moderate-temperature Domain T2, primary magmatic muscovite may be followed by primary magmatic andalusite. None of our samples shows an overgrowth of andalusite on muscovite, although such a textural relationship is not required. Finally, in the low-temperature Domain T3, the rocks contain magmatic muscovite, and potentially late subsolidus muscovite, but no magmatic andalusite.

Less favourable compositional conditions for crystallizing magmatic andalusite include restriction of the andalusite stability field (water-saturated solidus curve moves to higher temperature because of lower Al_2O_3, lower Be–B–Li–P–F, higher Ca, $a_{H2O} < 1$, etc.; the And = Sil curve moves to lower temperature because of lower minor constituents such as Fe; and the muscovite stability field expands as a result of Fe and F solubility). If Al_2O_3 decreases, the A/CNK composition of the melt is less favourable for crystallizing Al_2SiO_5, i.e. the AND MAX field shrinks as A/CNK $\rightarrow$1. With a much smaller stability field for andalusite, many more *P–T* crystallization paths for felsic magmas will not intersect it. For crystallization paths that do intersect the reduced andalusite field, only those with favourable compositional conditions of fractionation-enhanced or fluid-enhanced enrichment in A/CNK will attain Al_2SiO_5 saturation. Magmas with low A/CNK may pass through the entire *P–T* andalusite stability field, whatever its size, and never nucleate andalusite. For those cases in which fluid evolution can achieve critical saturation of Al_2SiO_5 in the melt, the *T–P* conditions must be below the water saturation curve (schematic heavy dashed line).

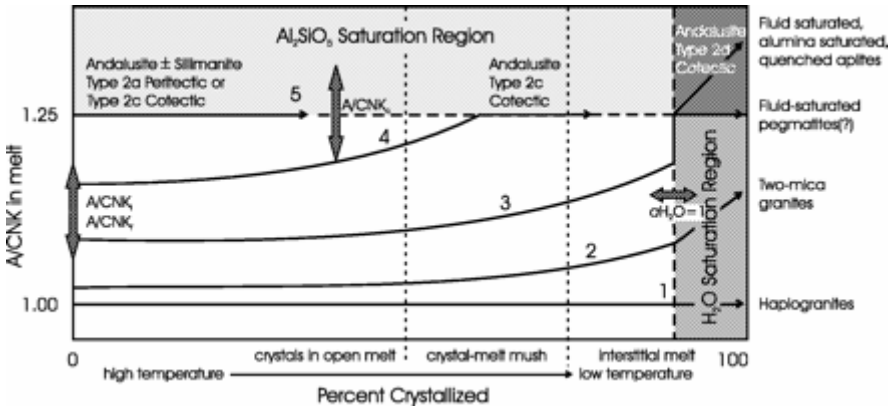


Fig. 15. Plot of A/CNK vs percent crystallization of haplogranitic and peraluminous melts. Double-headed arrows show the key system variables: $(A/CNK)_i$ of the melt and $(A/CNK)_f$ of the fractionating phases; $(A/CNK)_c$, the critical value of A/CNK required to saturate the melt in aluminosilicate; and $a_{H2O} = 1$, the point in the crystallization history at which the melt becomes saturated in water. Path 1 crystallizes only quartz and feldspar. Path 2 crystallizes micas as the mineralogical expression of the weak peraluminosity of the melt. Path 3 reaches Al_2SiO_5 saturation either by a combination of feldspar fractionation and water saturation, or by decrease in pressure causing a decrease in water and alumina solubility. Path 4 reaches Al_2SiO_5 saturation by feldspar fractionation alone. Path 5 is saturated in Al_2SiO_5 from the outset.

Figure 15 is a graphic summary of this view that the most important controls on the formation of magmatic andalusite are A/CNK and fluid saturation in the melt. It depicts five possible crystallization paths, three of which produce andalusite. The textural type of andalusite depends on whether the magma reaches Al_2SiO_5 saturation before water saturation (mainly textural types S1–S3), or water saturation before Al_2SiO_5 saturation (textural types C1–C3).

The precise paths depend on the assemblage of phases crystallizing and the sequence in which they appear. In detail, the crystallization paths, in order of increasing $(A/CNK)_i$, are as follows.

Path 1. Initial melt is haplogranitic [$(A/CNK)_i = 1$] and anhydrous. Feldspar fractionation leaves A/CNK unchanged in the residual melt, water saturation is never attained, and no andalusite forms.

Path 2. Initial melt is weakly peraluminous and water undersaturated. Fractionated magma does not reach saturation in aluminosilicate, but it does reach water saturation, and eventually becomes an ordinary two-mica granite.

Path 3. Initial melt is moderately peraluminous and water undersaturated. Cystallization of anhydrous phases raises the A/CNK of the melt, but the melt reaches water saturation before Al_2SiO_5 saturation. The evolution of an alkali-bearing fluid phase may provide the essential increase to A/CNK to drive the residual melt against, or even into, the aluminosilicate field resulting in

crystallization of andalusite. Alternatively, adiabatic decompression of the water-saturated melt would reduce the solubility and concentration of water in the melt, and decrease the threshold of Al_2SiO_5 saturation to encompass the melt composition, resulting in andalusite precipitation. In the first case, the melt enters the andalusite stability field, and in the second case, the andalusite stability field overtakes the melt composition. In either case, the result is crystallization of andalusite, probably as quench clusters.

Path 4. Initial melt is highly peraluminous and water undersaturated. It reaches aluminosilicate saturation by fractionation alone to form single grains of andalusite, and may later form andalusite from the evolved fluid phase.

Path 5. Initial melt is aluminosilicate saturated from the outset and water undersaturated. It can contain single andalusite (or sillimanite) grains that may be magmatic, or xenocrystic, or both.

According to this model, andalusites in peraluminous felsic igneous rocks are texturally and genetically bimodal: those magmas that reach Al_2SiO_5 saturation before water saturation contain single grains of andalusite; those magmas that reach water saturation before Al_2SiO_5 saturation (and Al_2SiO_5 saturation by water saturation), contain clusters of andalusite. Some rocks may contain both single andalusite grains and clusters of andalusite grains (e.g. when Path 4 or 5 above reaches water saturation). As discussed previously, sample JAM-03 (Fig. 13d), with S1 and C1 andalusites, may be a macrocosm for what happens in the final interstitial melt of crystallizing granites. The interstitial melt reaches water saturation, and the release of the water causes a small quench cluster of andalusite to form.

The formation of muscovite reaction rims is independent of the mode of andalusite formation. Both textural types of magmatic andalusite may develop a muscovite reaction rim, depending on the conditions prevailing when the system encounters the muscovite stability field. Monocrystalline muscovite rims may be magmatic, whereas polycrystalline muscovite rims may be subsolidus.

We conclude that, because most of our whole-rock samples have A/CNK values less than the experimentally determined values needed to saturate in Al_2SiO_5, and because the effects of fractionation of feldspars and (biotite + cordierite) counterbalance, many late residual melts probably reach Al_2SiO_5 saturation by evolving a fluid phase. Only the last (interstitial) melt fraction attains sufficiently high A/CNK to nucleate andalusite. Whether it is the escape of alkalis from the melt, or the reduction in alumina solubility in the melt, the effect is the same; namely, to saturate the melt in Al_2SiO_5 and to crystallize andalusite. This model for andalusite formation may explain why many andalusites occur as clusters in late interstitial patches surrounded by reaction rims of muscovite. It can also explain why many of the andalusite-bearing whole-rock compositions have lower A/CNK ratios than experimentally

determined values necessary for Al_2SiO_5 saturation. Finally, if a correlation exists between the appearance of andalusite and appearance of a fluid phase, the number of Type 2d water-saturated magmatic andalusites may be even greater than believed.

SUMMARY AND CONCLUSIONS

Occurrence of andalusite in felsic igneous rocks
Andalusite is an accessory mineral occurring in a wide range of peraluminous felsic igneous rocks, including volcanic rocks, aplites, granites (commonly only in spatially restricted regions of plutons), pegmatites, and anatectic migmatites. It can occur as single grains, or as clusters of grains, with or without overgrowths of muscovite. It is commonly subhedral, compatible in grain size with its host rock, has an iron-rich (0·1–1·7 wt % FeO) core, and is normally not associated with sillimanite.

Textural and chemical criteria for determining the origin of andalusite
Textural and chemical evidence for a magmatic origin is strong for volcanic, aplitic, pegmatitic, and migmatitic andalusites, but is equivocal for medium- to coarse-grained plutonic andalusites. We considered grain size, grain shape, textural relations with other minerals, inclusion relations, chemical compositions, chemical zoning, and chemical equilibria with other minerals as tests for determining the origin of andalusite in a given rock. In general, inclusion relations (other than melt inclusions) and andalusite chemical compositions (except possibly zoning patterns) are generally not useful criteria, but the other criteria are extremely useful in specific cases. The chemical-equilibrium-with-other-minerals test shows that many rocks have biotite–muscovite–apatite compositions that appear to be in equilibrium with each other, and with andalusite, suggesting that they all have the same magmatic origin.

Genetic classification of andalusite
We have proposed the following genetic classification of andalusite in felsic igneous rocks.

Type 1 Metamorphic

a. *in situ* prograde (resulting from thermal metamorphism of peraluminous granitic rocks);
b. retrograde (resulting from inversion of sillimanite);
c. xenocrystic (generally anhedral, many inclusions, spatial proximity to country rocks and/or pelitic xenoliths);

d. restitic (residua of partial melting, generally anhedral with inclusions of high-grade metamorphic minerals).

Type 2 Magmatic

a. peritectic (water-undersaturated, $T\uparrow$), subhedral to euhedral, associated with leucosomes in migmatites;
b. peritectic (water-undersaturated, $T\rightarrow$), subhedral to anhedral, as reaction rims on garnet or cordierite;
c. cotectic (water-undersaturated, $T\downarrow$), euhedral, grain-size compatibility with host rock, few inclusions;
d. pegmatitic (water-saturated, $T\downarrow$), large subhedral to euhedral grains, associated with aplite–pegmatite contacts or pegmatitic portion alone.

Type 3 Metasomatic
Water-saturated, magma-absent conditions; andalusite spatially related to structural discontinuities in the host rock, coincident replacement of feldspar and/or biotite, intergrowths with quartz.

Controls on the formation of andalusite
Of the many possible controls on the formation of andalusite (excess Al_2O_3, water concentration and fluid evolution, high Be–B–Li–P, high F, high Fe–Mn–Ti, and kinetic considerations), the two most important factors appear to be excess Al_2O_3 and the effect of releasing water (either to strip alkalis from the melt or to reduce alumina solubility in the melt).

Origin of andalusite
Our deductions about the origin of andalusite rest on a sample set that encompasses a wide range of andalusite-bearing felsic igneous rocks worldwide. The strongest evidence for a magmatic origin for andalusite includes grain-size compatibility (including fine-grained clusters), euhedral or quench shapes, melt inclusions, and equilibrium chemical compositions of coexisting phases. We believe that the majority of andalusite in peraluminous felsic igneous rocks is of magmatic origin and, therefore, a significant stability region exists for magmatic andalusite, delimited by the water-saturated granite solidus, the And = Sil reaction, and the stability field of muscovite. The size of the magmatic andalusite stability field can expand or contract depending on a number of compositional parameters and, thus, the reactions shown as discrete lines in Fig. 14 are in practice broad zones.

The strongest evidence for a xenocrystic origin for andalusite includes grain-size incompatibility, anhedral grain shapes, textural disequilibrium (reaction rims), and general matching of textural and chemical parameters with andalusite in the country rock. Xenocrysts of andalusite do occur, but they are not as common as magmatic ones. True restitic andalusite is probably rare because the region of significant generation of granitoid magma occurs at higher temperatures and pressures than permitted by the andalusite stability

field. Occurrences of metasomatic andalusite may represent only volumetrically small and special cases.

Partial melting of semi-pelitic material under high pressure in the middle to lower crust probably results in the formation of peraluminous granitic melts in equilibrium with garnet (± sillimanite), not andalusite (Green, 1976; Vielzeuf & Holloway, 1988). Ascent ($T\downarrow$ $P\downarrow$) of the magma may bring those melts into the stability field of andalusite. Alternatively, partial melting of pelitic material under lower pressures in the middle to upper crust results, in many cases, in the formation of andalusite in the same peritectic reaction that forms the peraluminous melt phase. Andalusite may be a normal primary magmatic mineral in some water-poor peraluminous magmas. Fractional crystallization of feldspars may increase the A/CNK ratio of the original magma to andalusite saturation and precipitate single cotectic grains of andalusite. Alternatively, the inevitable attainment of water-saturated conditions in the magma can also result in the precipitation of andalusite from the silicate melt. Escape of fluid, with consequent depletion of alkalis or reduction of Al-solubility in the melt, creates saturation or oversaturation in Al_2SiO_5. Continued release of aqueous fluid keeps driving the interstitial residual melt into the Al_2SiO_5 (over)saturation region, removing heat from the system, and resulting in the precipitation of quench clusters of optically discontinuous andalusite grains. Clustered andalusites are at least as common as individual grains, even more so in plutonic rocks.

Why do so many peraluminous granites not contain andalusite? The simplest answer is that the *T–P–X* conditions are thermodynamically or kinetically unfavourable. Either the bulk composition is right but it is not in the *T–P* stability field of andalusite, or *T–P* conditions are right, but the melt A/CNK is inappropriate, or both. Another possibility is that the AND MAX field is reduced (by raising the granite solidus, shifting the And = Sil curve to lower temperature, or expanding the Ms field), so that the AND MAX field shrinks and a normal two-mica granite is the result. Ultimately, magmatic andalusite can be completely lost in a magmatic peritectic reaction. Also, because most felsic melts reach saturation in an aqueous fluid phase, one effect of this fluid may be to replace previously crystallized andalusite grains, resulting in a rock in which monocrystalline and/or polycrystalline muscovite mantles the andalusites.

The analysis of andalusite origins presented in this paper (i.e. classification on textural and chemical criteria, definition of *T–P–X* space, examination of reactions, relation to genetic types) is readily adaptable to any AFM mineral (Bt, Ms, Crd, Grt, etc.) in peraluminous igneous rocks. The genetic types of origin will probably be similar, and the *T–P–X* stability regions will be different but overlap to some extent.

ACKNOWLEDGEMENTS

This paper has been many years in development, and during that time several people, including Gordon Brown, Andrew Henry, Robert MacKay, Llewellyn Pearce, and Monica Rampoldi, have provided invaluable technical and logistical support, for which we express our gratitude. More recently, Calvin Miller and Alberto Patiño Douce provided valuable detailed reviews that led to considerable improvements in the manuscript. In addition, Barrie Clarke acknowledges the essential support of a research grant from the Natural Sciences and Engineering Research Council of Canada.

REFERENCES

Abbott, R. N. & Clarke, D. B. (1979). Hypothetical liquid relationships in the subsystem Al_2O_3–FeO–MgO projected from quartz, alkali feldspar and plagioclase for $a(H_2O) = 1$. *Canadian Mineralogist* **17**, 549–560.

Acosta-Vigil, A., Pereira, M. D., Shaw, D. M. & London, D. (2001). Contrasting behaviour of boron during crustal anatexis. *Lithos* **56**, 15–31.

Acosta-Vigil, A., London, D., Dewers, T. A. & Morgan, G. B., VI (2002). Dissolution of corundum and andalusite in H_2O-saturated haplogranitic melts at 800°C and 200 MPa: constraints on diffusivities and the generation of peraluminous melts. *Journal of Petrology* **43**, 1885–1908.

Acosta-Vigil, A., London, D., Morgan, G. B., VI & Dewers, T. A. (2003). Solubility of excess alumina in hydrous granitic melts in equilibrium with peraluminous minerals at 700–800°C and 200 MPa, and applications of the aluminum saturation index. *Contributions to Mineralogy and Petrology* **146**, 100–119.

Barker, D. S. (1987). Rhyolites contaminated with metapelite and gabbro, Lipari, Aeolian Islands, Italy: products of lower crustal fusion or of assimilation plus fractional crystallization? *Contributions to Mineralogy and Petrology* **97**, 460–472.

Barrera, J. L., Bellido, F. & Klein, E. (1985). Contact metamorphism in synkinematic two-mica granites produced by younger granitic intrusions, Galicia, N.W. Spain. *Geologie en Mijnbouw* **64**, 413–422.

Bouloton, J. (1992). Mise en évidence de cordiérite héritée des terrains traversés dans le pluton granitique des Oulad Ouaslam (Jebilet, Maroc). *Canadian Journal of Earth Sciences* **29**, 658–668.

Bouloton, J., El Amrani, I. E., El Mouraouah, A. & Montel, J. M. (1991). Les xénolites hyperalumineux des granites, d'après l'exemple du pluton superficiel des Oulad Ouslam (Jebilet, Maroc). *Comptes Rendus de l'Académie des Sciences* **312**, 273–279.

Brigatti, M. F., Frigieri, P., Ghezzo, C. & Poppi, L. (2000). Crystal chemistry of Al-rich biotites coexisting with muscovites in peraluminous granites. *American Mineralogist* **85**, 436–448.

Castelli, D. & Lombardo, B. (1988). The Gophu La and Western Lunana granites: Miocene muscovite leucogranites of the Bhutan Himalaya. *Lithos* **21**, 211–225.

Cesare, B. (1994). Synmetamorphic veining: origin of andalusite-bearing veins in the Vedrette di Ries contact aureole, Eastern Alps, Italy. *Journal of Metamorphic Geology* **12**, 643–653.

Cesare, B. & Gómez-Pugnaire, M. T. (2001). Crustal melting in the Alborán domain: constraints from the xenoliths of the Neogene Volcanic Province. *Physics and Chemistry of the Earth, Part A* **26**(4–5), 255–260.

Cesare, B., Gómez-Pugnaire, M. T., Sanchez-Navas, A. & Grobety, B. (2002). Andalusite–sillimanite replacement (Mazarrón–SE Spain): microstructural and TEM study. *American Mineralogist* **87**, 433–444.

Cesare, B., Marchesi, C., Hermann, J. & Gómez-Pugnaire, M. T. (2003). Primary melt inclusions in andalusite from anatectic graphitic metapelites: implications for the Al_2SiO_5 triple point. *Geology* **31**, 573–576.

Chappell, B. W., White, A. J. R. & Williams, L. S. (1991). A transverse section through granites of the Lachlan Fold Belt. *Second Hutton Symposium on Granites and Related Rocks. Australian Bureau of Mineral Resources, Record 1991/22*.

Chorlton, L. B. & Martin, R. F. (1978). The effect of boron on the granite solidus. *Canadian Mineralogist* **16**, 239–244.

Clarke, D. B. (1981). The mineralogy of peraluminous granites: a review. *Canadian Mineralogist* **19**, 3–17.

Clarke, D. B. & Bogutyn, P. A. (2003). Oscillatory epitactic-growth zoning in biotite and muscovite from the Lake Lewis leucogranite, South Mountain Batholith, Nova Scotia, Canada. *Canadian Mineralogist* **41**, 1027–1047.

Clarke, D. B., McKenzie, C. B., Muecke, G. K. & Richardson, S. W. (1976). Magmatic andalusite from the South Mountain Batholith, Nova Scotia. *Contributions to Mineralogy and Petrology* **56**, 279–287.

Clarke, D. B., Henry, A. S. & White, M. A. (1998). Exploding xenoliths and the absence of 'elephants' graveyards' in granite batholiths. *Journal of Structural Geology* **20**, 1325–1343.

Clarke, D. B., MacDonald, M. A. & Erdmann, S. (2004). Chemical variation in Al_2O_3–CaO–Na_2O–K_2O space: controls on the peraluminosity of the South Mountain Batholith. *Canadian Journal of Earth Sciences* **41**, 785–798.

Clemens, J. D. & Wall, V. J. (1981). Origin and crystallization of some peraluminous (S-type) granitic magmas. *Canadian Mineralogist* **19**, 111–131.

Clemens, J. D. & Wall, V. J. (1988). Controls on the mineralogy of S-type volcanic and plutonic rocks. *Lithos* **21**, 53–66.

Corey, M. C. (1988). An occurrence of metasomatic aluminosilicates related to high alumina hydrothermal alteration within the South Mountain Batholith, Nova Scotia. *Maritime Sediments and Atlantic Geology* **24**, 83–95.

D'Amico, C., Rottura, A., Bargossi, G. M. & Nannetti, M. C. (1982–1983*a*). Magmatic genesis of andalusite in peraluminous granites. Examples from Eisgarn type granites in Moldanubikum. *Rendiconti della Società Italiana di Mineralogia e Petrologia* **38**, 15–25.

D'Amico, C., Rottura, A., Maccarrone, E. & Puglisi, G. (1982–1983*b*). Peraluminous granitic suite of Calabria–Peloritani arc. *Rendiconti della Società Italiana di Mineralogia e Petrologia* **38**, 35–52.

Deer, W. A., Howie, R. A. & Zussman, J. (1982). *Rock-Forming Minerals, Vol. 1A, Orthosilicates*, 2nd edn. Harlow: Longman.

Didier, J. (1991). The main types of enclaves in the Hercynian granitoids of the Massif Central, France. In: Didier, J. & Barbarin, B. (eds) *Enclaves and Granite Petrology*. Amsterdam: Elsevier, pp. 47–61.

Ellis, D. J. & Obata, M. (1992). Migmatite and melt segregation at Cooma, New South Wales. *Transactions of the Royal Society of Edinburgh: Earth Sciences* **83**(1–2), 95–106.

Evensen, J. M., London, D. & Wendlandt, R. F. (1999). Solubility and stability of beryl in granitic melts. *American Mineralogist* **84**, 733–745.

Fernández-Catuxo, J., Corretgé, L. G. & Suárez, O. (1995). Influencia de los elementos menores en la estabilidad de la andalucita en rocas graníticas del Macizo Ibérico. *Boletín de la Sociedad Española de Mineralogía* **18**, 55–71.

Ferrow, E. A., London, D., Goodman, K. S. & Veblen, D. R. (1990). Sheet silicates of the Lawler Peak granite, Arizona: chemistry, structural variations, and exsolution. *Contributions to Mineralogy and Petrology* **105**, 491–501.

Gaspar, L. M. & Inverno, C. M. C. (1998). P-enriched peraluminous leucogranites in Barca de Alva–Escalhao, NE Portugal. A multi-stage anatectic complex. *Acta Universitatis Carolinae—Geologica* **42**, 35–40.

Grambling, J. A. & Williams, M. L. (1985). The effect of Fe^{3+} and Mn^{3+} on aluminum silicate phase relations in north–central New Mexico, U.S.A. *Journal of Petrology* **26**, 324–354.

Green, T. H. (1976). Experimental generation of cordierite- or garnet-bearing granitic liquids from a pelitic composition. *Geology* **4**, 85–88.

Greenwood, H. J. (1976). Metamorphism at moderate temperatures and pressures. In: Bailey, D. K. & MacDonald, R. (eds) *The Evolution of the Crystalline Rocks*. London: Academic Press, pp. 187–259.

Halliday, A. N., Stephens, W. E. & Harmon, R. S. (1981). Isotopic and chemical constraints on the development of peraluminous Caledonian and Acadian granites. *Canadian Mineralogist* **19**, 205–216.

Hills, E. S. (1938). Andalusite and sillimanite in uncontaminated igneous rocks. *Geological Magazine* **75**, 296–304.

Holdaway, M. J. (1971). Stability of andalusite and the aluminosilicate phase diagram. *American Journal of Science* **271**, 97–131.

Holdaway, M. J. & Mukhopadhyay, B. (1993). A re-evaluation of the stability relations of andalusite: thermochemical data and phase diagram for the aluminum silicate. *American Mineralogist* **78**, 298–315.

Holland, T. & Powell, R. (1985). An internally consistent thermodynamic data set with uncertainties and correlations: 2. Data and results. *Journal of Metamorphic Geology* **3**, 343–370.

Holland, T. & Powell, R. (2001). Calculation of phase relations involving haplogranitic melts using an internally consistent thermodynamic dataset. *Journal of Petrology* **42**, 673–683.

Hollister, L. S. & Bence, A. E. (1967). Staurolite: sector compositional variations. *Science* **158**, 1053–1056.

Holtz, F., Johannes, W. & Pichavant, M. (1992). Peraluminous granitoids: the effect of alumina on melt composition and coexisting minerals. *Transactions of the Royal Society of Edinburgh, Earth Sciences* **86**, 409–416.

Icenhower, J. P. & London, D. (1995). An experimental study of element partitioning among biotite, muscovite, and coexisting peraluminous silicic melt at 200 MPa (H_2O). *American Mineralogist* **80**, 1229–1251.

Johannes, W. (1978). Melting of plagioclase in the system Ab–An–H_2O and Qz–Ab–An–H_2O at $P(H_2O)$ = 5 kbars, an equilibrium problem. *Contributions to Mineralogy and Petrology* **66**, 295–303.

Johannes, W. & Holtz, F. (1996). *Petrogenesis and Experimental Petrology of Granitic Rocks*. Berlin: Springer, 335 pp.

Johnson, S. E. & Vernon, R. H. (1995). Stepping stones and pitfalls in the determination of an anticlockwise *P–T–t*–deformation path: the low-*P*, high-*T* Cooma Complex, Australia. *Journal of Metamorphic Geology* **13**, 165–183.

Johnson, T. E., Brown, M. & Solar, G. S. (2003). Low-pressure subsolidus and suprasolidus phase equilibria in the MnNCKFMASH system: constraints on conditions of regional metamorphism in western Maine, northern Appalachians. *American Mineralogist* **88**, 624–638.

Joyce, D. B. & Voigt, D. E. (1994). A phase equilibrium study in the system $KAlSi_3O_8$–$NaAlSi_3O_8$–SiO_2–Al_2SiO_5–H_2O and petrogenetic implications. *American Mineralogist* **79**, 504–512.

Kawakami, T. (2001). Boron depletion accompanied by the breakdown of tourmaline in the migmatite-zone of the Aoyama area, Ryoke metamorphic belt, SW Japan; an implication for the formation of tourmaline leucogranites. *Geological Society of America, Abstracts with Programs* **33**(6), 330.

Kawakami, T. (2002). Magmatic andalusite from the migmatite zone of the Aoyama area, Ryoke metamorphic belt, SW Japan, and its importance in constructing the *P–T* path. *Journal of Mineralogical and Petrological Sciences* **97**, 241–254.

Kerrick, D. M. (1990). *The Al_2SiO_5 Polymorphs. Mineralogical Society of America, Reviews in Mineralogy* **22**.

Kerrick, D. M. & Speer, J. A. (1988). The role of minor element solid solution on the andalusite–sillimanite equilibrium in metapelites and peraluminous granitoids. *American Journal of Science* **288**(2), 152–192.

Kontak, D. J., Martin, R. F. & Richard, L. (1996). Patterns of phosphorus enrichment in alkali feldspar, South Mountain Batholith, Nova Scotia, Canada. *European Journal of Mineralogy* **8**, 805–824.

Kretz, R. (1983). Symbols for rock-forming minerals. *American Mineralogist* **68**, 277–279.

Kriegsman, L. M. (2001). Partial melting, partial melt extraction and partial back reaction in anatectic migmatites. *Lithos* **56**, 75–96.

Larson, T. & Sharp, Z. (2003). Stable isotope constraints on the Al_2SiO_5 'triple-point' rocks from the Proterozoic Priest pluton contact aureole, New Mexico. *Geological Society of America, Abstracts with Programs* **33**(5), 11.

Leal Gomes, C. (1984). Ocorrencia de andaluzite em pegmatitos da região de Arreigada, Paços de Ferreira, Porto. *Memorias e Noticias, Publicacoes do Museu e Laboratorio Mineralogico e Geologico de Universidade de Coimbra* **98**, 175–194.

London, D. & Burt, D. M. (1982). Chemical models for lithium aluminosilicate stabilities in pegmatites and granites. *American Mineralogist* **67**, 494–509.

London, D., Hervig, R. L. & Morgan, G. B., VI (1988). Melt–vapor solubilities and elemental partitioning in peraluminous granite–pegmatite systems; experimental results with Macusani glass at 200 MPa. *Contributions to Mineralogy and Petrology* **99**, 360–373.

London, D., Wolf, M. B., Morgan, G. B., VI & Garrido, M. G. (1999). Experimental silicate–phosphate equilibria in peraluminous granitic magmas, with a case study of the Alburquerque batholith at Tres Arroyos, Badajoz, Spain. *Journal of Petrology* **40**, 215–240.

London, D., Morgan, G. B., VI & Wolf, M. B. (2001). Amblygonite montebrasite solid solutions as monitors of fluorine in evolved granitic and pegmatitic melts. *American Mineralogist* **86**, 225–233.

López Ruiz, J. & Rodríguez Badiola, E. (1980). La región volcánica neógena del sureste de España. *Estudios Geológicos* **36**, 5–63.

Lowenstern, J. B. & Sinclair, W. D. (1996). Exsolved magmatic fluid and its role in the formation of comb-layered quartz at the Cretaceous Logtung W–Mo deposit, Yukon Territory, Canada. *Geological Society of America, Special Papers* **315**, 291–303.

Manning, D. A. C. & Pichavant, M. (1983). The role of fluorine and boron in the generation of granitic melts. In: Atherton, M. P. & Gribble, C. D. (eds) *Migmatites, Melting and Metamorphism*. Nantwich: Shiva, pp. 94–109.

Martin, J. S. & Henderson, C. M. B. (1984). An experimental study of the effects of small amounts of lithium on the granite system. *Progress in Experimental Petrology* **6**, 30–35.

Messina, A., Russo, S., Perrone, V. & Giacobbe, A. (1991). Geological and petrochemical study of the Sila Massif plutonic rocks (Northern Calabria, Italy). *Bollettino della Societa Geologica Italiana* **110**, 165–206.

Miller, C. F., Stoddard, E. F., Bradfish, L. J. & Dollase, W. A. (1981). Composition of plutonic muscovite: genetic implications. *Canadian Mineralogist* **19**, 25–34.

Monier, G., Mergoil-Daniel, J. & Labernardiere, H. (1984). Générations successives de muscovites et feldspaths potassiques dans les leucogranite du massif de Millevaches (Massif Central français). *Bulletin de Minéralogie* **107**, 55–68.

Montel, J. M., Didier, J. & Pichavant, M. (1991). Origin of surmicaceous enclaves in intrusive granites. In: Didier, J. & Barbarin, B. (eds) *Enclaves and Granite Petrology*. Amsterdam: Elsevier, pp. 509–528.

Morgan, G. B., VI, London, D. & Luedke, R. G. (1998). Petrochemistry of late Miocene peraluminous silicic volcanic rocks from the Morococala field, Bolivia. *Journal of Petrology* **39**, 601–632.

Neves, L. J. P. F. (1997). Trace element content and partitioning between biotite and muscovite of granitic rocks: a study in the Viseu region (central Portugal). *European Journal of Mineralogy* **9**, 849–857.

Neves, L. J. P. F., Godinho, M. M. & Pereira, A. J. S. C. (1999). O filão leucogranitico de Borralhal–Salgueiral (Viseu, Portugal Central): uma rocha HHP rica em fósforo e geoquimicamente especializada. *Comunicacoes do Instituto Geologico e Mineiro* **86**, 15–24.

Patiño Douce, A. E. (1992). Calculated relationships between activity of alumina and phase assemblages of silica-saturated igneous rocks; petrogenetic implications of magmatic cordierite, garnet and aluminosilicate. *Journal of Volcanology and Geothermal Research* **52**, 43–63.

Pattison, D. R. M. (1992). Stability of andalusite and sillimanite and the Al_2SiO_5 triple point: constraints from the Ballachulish aureole, Scotland. *Journal of Geology* **100**, 423–446.

Pattison, D. R. M. (2001). Instability of Al_2SiO_5 'triple-point' assemblages in muscovite + biotite + quartz-bearing metapelites, with implications. *American Mineralogist* **86**, 1414–1422.

Pattison, D. R. M. & Tracy, R. J. (1991). Phase equilibria and thermobarometry of metapelites. In: Kerrick, D. M. (ed.) *Contact Metamorphism. Mineralogical Society of America, Reviews in Mineralogy* **26**, 105–206.

Pattison, D. R. M., Spear, F. S., DeBuhr, C. L., Cheney, J. T. & Guidotti, C. V. (2002). Thermodynamic modelling of the reaction muscovite + cordierite = Al_2SiO_5 + biotite + quartz + H_2O; constraints from natural assemblages and implications for the metapelitic petrogenetic grid. *Journal of Metamorphic Geology* **20**, 99–118.

Pichavant, M. & Manning, D. (1984). Petrogenesis of tourmaline granites and topaz granites; the contribution of experimental data. *Physics of the Earth and Planetary Interiors* **35**, 31–50.

Pichavant, M., Kontak, D. J., Herrera, J. V. & Clark, A. H. (1988). The Miocene–Pliocene Masucani volcanics, SE Peru I. Mineralogy and magmatic evolution of a two-mica aluminosilicate-bearing ignimbrite suite. *Contributions to Mineralogy and Petrology* **100**, 300–324.

Rapela, C. W., Baldo, E. G., Pankhurst, R. J. & Saavedra, J. (2002). Cordieritite and leucogranite formation during emplacement of highly peraluminous magma; the El Pilon granite complex (Sierras Pampeanas, Argentina). *Journal of Petrology* **43**, 1003–1028.

Richardson, S. W., Gilbert, M. C. & Bell, P. M. (1969). Experimental determination of kyanite–andalusite and andalusite–sillimanite equilibria; the aluminum silicate triple point. *American Journal of Science* **267**, 259–272.

Rottura, A., Caggianelli, A., Campana, R. & Del Moro, A. (1993). Petrogenesis of Hercynian peraluminous granites from the Calabrian Arc, Italy. *European Journal of Mineralogy* **5**, 737–754.

Salje, E. (1986). Heat capacities and entropies of andalusite and sillimanite: the influence of fibrolitization on the phase diagram of the Al_2SiO_5 polymorphs. *American Mineralogist* **71**, 1366–1371.

Scaillet, B., Pichavant, M. & Roux, J. (1995). Experimental crystallization of leucogranite magmas. *Journal of Petrology* **36**, 663–705.

Shiba, M. (1988). Metamorphic evolution of the southern part of the Hidaka belt, Hokkaido, Japan. *Journal of Metamorphic Geology* **6**, 273–296.

Spear, F. S., Kohn, M. J. & Cheney, J. T. (1999). *P–T* paths from anatectic pelites. *Contributions to Mineralogy and Petrology* **134**, 17–32.

Tinkham, D. K., Zuluaga, C. A. & Stowell, H. H. (2001). Metapelite phase equilibria modelling in MnNCKFMASH: the effect of variable Al_2O_3 and MgO/(MgO + FeO) on mineral stability. *Geological Materials Research* **3**(1).

Tischendorf, G., Gottesmann, B., Förster, H.-J. & Trumbull, R. B. (1997). On Li-bearing micas: estimating Li from electron microprobe analyses and an improved diagram for graphical representation. *Mineralogical Magazine* **61**, 809–834.

Tischendorf, G., Förster, H.-J. & Gottesmann, B. (1999). The correlation between lithium and magnesium in trioctahedral micas: improved equations for Li_2O estimation from MgO data. *Mineralogical Magazine* **63**, 57–74.

Tuttle, O. F. & Bowen, N. L. (1958). *Origin of Granite in the Light of Experimental Studies in the System $NaAlSi_3O_8$–$KAlSi_3O_8$–SiO_2–H_2O. Geological Society of America, Memoir* **74**.

Vernon, R. H. (1982). Isobaric cooling of two regional metamorphic complexes related to igneous intrusions in Southeastern Australia. *Geology* **10**, 76–81.

Vernon, R. H. & Collins, W. J. (1988). Igneous microstructures in migmatites. *Geology* **16**, 1126–1129.

Vernon, R. H., Clarke, G. L. & Collins, W. J. (1990). Local, mid-crustal granulite facies metamorphism and melting: an example in the Mount Stafford area, central Australia. In: Ashworth, J. R. & Brown, M. (eds) *High-temperature Metamorphism and Crustal Anatexis*. London: Unwin Hyman, pp. 272–315.

Vielzeuf, D. & Holloway, J. R. (1988). Experimental determination of the fluid-absent melting relations in the pelitic system. *Contributions to Mineralogy and Petrology* **98**, 257–276.

Visonà, D. & Lombardo, B. (2002). Two-mica and tourmaline leucogranites from the Everest–Makalu region (Nepal–Tibet). Himalayan leucogranite genesis by isobaric heating? *Lithos* **62**, 125–150.

Voloshin, A. V. & Davidenko, I. V. (1973). Andalusite in granite pegmatites of the Kola Peninsula. *Transactions (Doklady) of the USSR Academy of Sciences, Earth Science Sections* **203**, 116–117.

Walker, R. J., Hanson, G. N. & Papike, J. J. (1989). Trace element constraints on pegmatite genesis: Tin Mountain pegmatite, Black Hills, South Dakota. *Contributions to Mineralogy and Petrology* **101**, 290–300.

Wall, V. J., Clemens, J. D. & Clarke, D. B. (1987). Models for granitoid evolution and source compositions. *Journal of Geology* **95**, 731–749.

Webster, J. D. (1997). Chloride solubility in felsic melts and the role of chloride in magmatic degassing. *Journal of Petrology* **38**, 1793–1807.

Whitney, D. L. & Dilek, Y. (2000). Andalusite–sillimanite–quartz veins as indicators of low-pressure–high-temperature deformation during late-stage unroofing of a metamorphic core complex, Turkey. *Journal of Metamorphic Geology* **18**, 59–66.

Wyllie, P. J. & Tuttle, O. F. (1964). Experimental investigations of silicate systems containing two volatile components. Part 3. The effects of SO_3, P_2O_5, HCl, and Li_2O in addition to H_2O on the melting temperature of albite and granite. *American Journal of Science* **262**, 930–939.

Yokoi, K. (1983). Fe_2O_3 contents of co-existing andalusite and sillimanite in the Ryoke metamorphic rocks occurring in the Hiraoka–Kadoya area, central Japan. *Journal of the Japanese Association of Mineralogists, Petrologists and Economic Geologists* **78**, 246–254.

Zaleski, E. (1985). Regional and contact metamorphism within the Moy Intrusive Complex, Grampian Highlands, Scotland. *Contributions to Mineralogy and Petrology* **89**, 296–306.

Zen, E-an (1988). Phase relations of peraluminous granitic rocks and their petrogenetic implications. *Annual Review of Earth and Planetary Sciences* **16**, 21–51.

Zen, E-an (1989). Wet and dry AFM mineral assemblages of strongly peraluminous granites. *EOS Transactions, American Geophysical Union* **70**, 109–110.